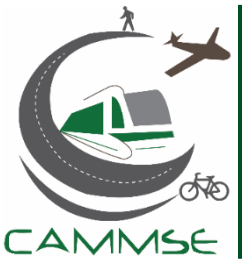

Center for Advanced Multimodal Mobility Solutions and Education

Project ID: 2019 Project 17

DYNAMIC SPEED HARMONIZATION IN CONNECTED URBAN STREET NETWORKS: IMPROVING MOBILITY

Final Report

by

Ali Hajbabaie, Ph.D. (ORCID ID: https://orcid.org/0000-0001-6757-1981)
North Carolina State University

Mehrdad Tajalli (ORCID ID https://orcid.org/0000-0002-4161-7344)
North Carolina State University

for

Center for Advanced Multimodal Mobility Solutions and Education
(CAMMSE @ UNC Charlotte)
The University of North Carolina at Charlotte
9201 University City Blvd
Charlotte, NC 28223

September 2020

ACKNOWLEDGEMENTS

The authors would like to thank the CAMMSE University Transportation Center and the Department of Civil and Environmental Engineering at Washington State University for their financial support of this research project.

DISCLAIMER

Table of Contents

EXCUTIVE SUMMARY ..... **vi**
CHAPTER 1. INTRODUCTION **1**
1.1 PROBLEM STATEMENT 1
1.2 RESEARCH OBJECTIVES 1
1.3 CONTRIBUTION OF RESEARCH 2
1.4 REPORT OVERVIEW 2
CHAPTER 2. LITERATURE REVIEW **3**
2.1 INTRODUCTION 3
2.2 SPEED HARMONIZATION IN FREEWAY FACILITIES 3
2.3 DYNAMIC SPEED HARMONIZATION IN ARTERIAL STREETS 4
2.4 DYNAMIC SPEED HARMONIZATION IN URBAN NETWORKS 4
2.5 COORDINATED SIGNAL TIMING AND SPEED HARMONIZATION 5
2.6 STRATEGIES TO REDUCE THE COMPUTATIONAL COMPLEXITY OF TRAFFIC CONTROL PROBLEMS 5
2.6.1 DECOMPOSITION APPROACHES FOR TRAFFIC CONTROL 6
2.6.2 DISTRIBUTED OPTIMIZATION AND COORDINATION ALGORITHMS (DOCA) FOR TRAFFIC CONTROL 6
2.7 SUMMARY 6
CHAPTER 3. PROBLEM FORMULATION **7**
3.1 INTRODUCTION 7
3.2 SPEED HARMONIZATION PROBLEM 7
3.3 LINEAR SPEED CONTROL 10
3.4 COOPERATIVE SIGNAL TIMING AND SPEED HARMONIZATION 12
CHAPTER 4. REAL-TIME SOLUTIONS FOR DYNAMIC SPEED HARMONIZATION PROBLEM INTRODUCTION **13**
4.1 INTRODUCTION 13
4.2 DISTRIBUTED OPTIMIZATION 13
4.3 DISTRIBUTED COORDINATION 16
4.4 DOCA-DSH FRAMEWORK 18
CHAPTER 5. CASE STUDY AND NUMERICAL RESULTS **19**
5.1 CASE STUDY NETWORK 19
5.2 IMPLEMENTATION OF THE ALGORITHM IN VISSIM 20
5.3 ANALYSIS SCENARIOS 21
5.4 DYNAMIC SPEED HARMONIZATION PERFORMANCE 21
5.5 COORDINATED SIGNAL TIMING AND SPEED HARMONIZATION PERFORMANCE 28
CHAPTER 6. SUMMARY AND CONCLUSIONS **33**
REFERENCES **34**

List of Figures

FIGURE 3.1: FUNDAMENTAL DIAGRAM OF TRAFFIC FLOW IN CTM. 9
FIGURE 3.2: LINEARIZING SPEED DIFFERENCES USING TRAFFIC FLOW FUNDAMENTAL DIAGRAM ... 11
FIGURE 4.1: DECOMPOSITION OF TWO-INTERSECTION NETWORK 14
FIGURE 4.2: INFORMATION FLOW IN DISTRIBUTED OPTIMIZATION AND COORDINATION 18
FIGURE 5.1: DOWNTOWN SPRINGFIELD, ILLINOIS THAT IS USED AS THE CASE STUDY NETWORK ... 19
FIGURE 5.2: TIME-VARIANT DEMAND PROFILE 20
FIGURE 5.3: VISSIM COM INTERFACE TO APPLY THE OPTIMIZED SIGNAL TIMINGS AND SPEEDS 21
FIGURE 5.4: THE COMPARISON OF SPEED VARIATIONS ON THE NETWORK WITH DIFFERENT DEMAND PATTERNS 22
FIGURE 5.5: DISTRIBUTION OF THE AVERAGE SPEED OVER THE NETWORK 24
FIGURE 5.6: THE RELATIONSHIP BETWEEN TRAVEL TIME, AVERAGE SPEED, AND SPEED VARIANCE IN THE NETWORK WITH ALPHA 25
FIGURE 5.7: OBJECTIVE VALUES FOR DIFFERENT DEMAND PATTERNS IN THE NETWORK WITH 20 INTERSECTIONS (×105) 26
FIGURE 5.8: THE OPTIMALITY GAP FOR THE NETWORKS WITH DIFFERENT SIZES WITH A STUDY PERIOD OF 250 TIME STEPS 27
FIGURE 5.9: THE OPTIMALITY GAP FOR THE NETWORKS WITH DIFFERENT SIZES WITH A STUDY PERIOD OF 500 TIME STEPS 27
FIGURE 5.10: AVERAGE RUNTIMES OF SUBPROBLEMS 28
FIGURE 5.11: VEHICLES TRAJECTORIES 30
FIGURE 5.12: OPTIMAL SIGNAL TIMING PARAMETERS AT INTERSECTION 19 31
FIGURE 5.13: DOCA AND THE BENCHMARK SOLUTIONS OBJECTIVE VALUES FOR THREE DEMAND PATTERNS 31
FIGURE 5.14: DOCA RUNTIMES AT EACH INTERSECTION NODE. 32

List of Tables

TABLE 3.1: SUMMARY OF NOTATIONS 7
TABLE 5.1: CHARACTERISTICS OF SPRINGFIELD NETWORK IN CTM 20
TABLE 5.2: MOBILITY PERFORMANCE OF THE NETWORK 26
TABLE 5.3: TOTAL RUNTIMES (SECOND) FOR DIFFERENT SIZES AND STUDY PERIODS WHEN DEMAND IS 900 VEH/HOUR/LANE 28
TABLE 5.4: COMPARING THE AVERAGE RUNTIMES (SECONDS) FOR ONE, TWO, AND THREE INTERSECTION-BASED SUBPROBLEMS 28
TABLE 5.5: THE NETWORK MOBILITY PERFORMANCES FOR THREE SCENARIOS AND THREE DEMAND PATTERNS BASED ON VISSIM 29

EXCUTIVE SUMMARY

Dynamic speed harmonization (DHS) is a traffic congestion management technique that can improve mobility and safety in transportation networks. It can regulate traffic flow by controlling vehicle speeds and prevent congestion and gridlocks. In particular, optimizing the speed of connected automated vehicles (CAVs) can adjust their arrival time and speed at intersections and significantly reduce the number of stops. However, the computational complexity of dynamic speed harmonization, especially in large-sized transportation networks, discourages its real-world applications. Hence, this research aims at developing an efficient and effective speed control algorithm that improves mobility in connected urban street networks in real-time.

The introduced speed harmonization strategy in this research aims at minimizing the temporal and spatial variations in speed while maximizing the network throughput. This research developed an analytical mathematical program and introduced a technique that uses the fundamental traffic flow diagram to solve the problem efficiently. Furthermore, a Distributed Optimization and Coordination Algorithm (DOCA) is developed to ensure that speed harmonization works in real-time. DOCA decomposes the network-level problem into several subproblems to reduce computational complexity. Moreover, establishing effective coordination among subproblems pushes suboptimal solutions towards global optimality. Results in a network of 20 intersections showed reductions in the total travel time and number of stops by up to 5.4% and 29.4%, respectively. Besides, the solutions were found in real-time with a 2.7% maximum optimality gap.

This study integrated signal control in the speed harmonization algorithm to further improve traffic operations. Results showed that coordinated signal timing and speed optimization algorithm reduced the average delay by 5.3% and the average number of stops by 28.5% when compared with independent signal timing optimization in a network of 20 intersections.

Chapter 1. Introduction

Emerging connectivity and automation technologies can be utilized in traffic control systems to improve mobility in transportation networks. Speed harmonization, powered by connectivity and automation technologies, can reduce traffic congestion on urban street networks similar to its observed promising impacts in freeway facilities. For instance, optimal speeds can be assigned to individual vehicles approaching an intersection to facilitates their arrival during the green signal and consequently avoid stops (He, Liu and Liu, 2015). As Zhu and Ukkusuri (2014a) showed, dynamic speed limit control in a connected vehicle environment could reduce total travel time by 18% and emissions by 20%.

In this project, we aim at developing a mathematical program for dynamic speed harmonization in large-sized transportation networks. We also integrate the signal timing optimization into speed harmonization and study how mobility can be improved further.

1.1 Problem Statement

Several studies have shown the effectiveness of speed harmonization in improving traffic operations; however, they were tested in simplified networks due to the complexity of speed harmonization. It is essential to show the effectiveness of this strategy in a complex network setting with high traffic demand levels by developing an efficient and accurate optimization and prediction model.

This project presents a novel methodology to harmonize the speed of CAVs in urban street networks. The methodology is based on a multi-objective optimization program and includes an algorithm to determine advisory speeds in network links dynamically. A mathematical program is developed and linearized using fundamental traffic flow concepts for this purpose. We also take into account stochastic traffic demands and capacities by embedding DSH into a Model Predictive Control (MPC) framework. Finally, we will study the proposed methodology from a microscopic perspective using Vissim (PTV Group, 2013).

1.2 Research Objectives

The goal of this project is to improve mobility in urban street networks by developing a methodology for dynamic speed harmonization suitable for connected urban street networks. The methodology aims at finding optimal advisory speeds on each transportation link that will be transferred to connected and autonomous vehicles, with the objective of reducing travel time, improving mobility, and harmonizing the speeds at the same time. As such, the methodology can avoid long queues, queue spillovers, and gridlocks. This study will generate the first network-level formulation for dynamic speed harmonization in a signalized network. It will also incorporate connected vehicle information in the mathematical model and the proposed solution algorithm.

The objective of this research is to study the effects of harmonizing the speed of connected automated vehicles on traffic operations in urban street networks. In particular, this study proposes the use of optimal speed control methods to develop an efficient optimization framework for an effective and fluent movement of CAVs in urban street networks. This study aimed at finding answers to the following fundamental research questions:

What is the effect of speed control on the operational performance of connected urban street networks?

How cooperative optimization of signal timing plans and speed of CAVs further improves the performance of transportation networks?

1.3 Contribution of Research

An efficient methodology is required to dynamically control the movement of connected and automated vehicles in urban street networks. However, most of the existing studies focus on static traffic models, which are not responsive to dynamic traffic changes. Therefore, the effect of speed harmonization could not be evaluated accurately in transportation networks. This research develops a novel multi-objective optimization program as well as analytical solution techniques to dynamically control vehicles' speeds to provide smooth movement of vehicles on urban street networks.

Moreover, signal timing optimization is incorporated into speed harmonization. Cooperative signal timing and speed optimization can improve traffic operations further. Existing studies showed the effectiveness of cooperative signal and speed optimization only in small networks due to its computational complexity. This study addresses the knowledge gap and provides more insight into the effects of cooperative signal timing and speed optimization in large scale transportation networks.

1.4 Report Overview

This report includes six chapters. An extensive literature review on existing speed harmonization approaches is discussed in Chapter 2. The mathematical formulation of the speed harmonization program in addition to coordinated signal timing and speed harmonization is detailed in Chapter 3. Chapter 4 provides a distributed optimization and coordination algorithm designed for large-sized urban street networks. Numerical results are provided in Chapter 5 to show the impacts of dynamic speed harmonization on network performance. Moreover, the discussion on the optimality gap, solution runtime, and the overall performance of the distributed approach is presented in this chapter. Finally, Chapter 6 provides a summary of the key findings.

Chapter 2. Literature Review

2.1 Introduction

This chapter presents an extensive review of the available speed harmonization approaches. These approaches are categorized into speed harmonization in freeway facilities, arterial streets, and urban networks. In addition, the studies on cooperative signal timing and speed harmonization are covered. We also describe traffic congestion management studies that used decomposition and distributed techniques to reduce the complexity of traffic modeling and optimization. The details of each category follow.

2.2 Speed harmonization in freeway facilities

Emerging connectivity and automation technologies can be utilized in traffic control systems to improve mobility in transportation networks. Finding proper signal timing parameters (Hajbabaie and Benekohal, 2011; He, Head and Ding, 2014; Feng et al., 2015; Mohebifard and Hajbabaie, 2019; Islam, Aziz and Hajbabaie, 2020; Tajalli, Mehrabipour and Hajbabaie, 2020), optimizing traffic metering rates on freeway facilities or urban street networks metering (Hajbabaie and Rahim Benekohal, 2011; Medina, Hajbabaie and Benekohal, 2013; Ntousakis, Nikolos and Papageorgiou, 2016; Letter and Elefteriadou, 2017; Mohebifard and Hajbabaie, 2018, 2019a; Mohebifard, Islam and Hajbabaie, 2019; Hajbabaie and Mohebifard, 2020), performing traffic assignment (Hajibabai, Bai and Ouyang, 2014; Zhu and Ukkusuri, 2015; Levin and Boyles, 2016; Mehrabipour, Hajibabai and Hajbabaie, 2019), and optimizing the speed of connected automated vehicles in intersections (Mirheli, Hajibabai and Hajbabaie, 2018; Tajalli and Hajbabaie, 2018b, 2018a; Mirheli *et al.*, 2019; Niroumand *et al.*, 2020a, 2020b) are examples of well-known strategies that reduce urban traffic congestion.

Several studies considered the effects of variable speed limit (VSL) on safety, environmental, and mobility measures in freeway facilities. The initial purpose of VSL was to improve safety in work zones and under inclement weather conditions (Robinson, 2000). VSL can reduce the speed limit upstream of a crash-prone location and increase it downstream of that location (Abdel-Aty, Dilmore and Dhindsa, 2006). VSL is shown to increase the average headway and to decrease speed mean and variance (Ha, Kang and Park, 2003). Thus, it can reduce the number and severity of crashes (Smulders, 1990). In addition, VSL provides smoother traffic flow, where the number of lane changing maneuvers is reduced in congested conditions (Borrough, 1997). It is shown that there is a direct relationship between the CO emissions and the vehicles' speed on roads (Aziz & Ukkusuri 2012). Implementing VSL on the M42 highway in the UK showed emission reductions between 4 to 10 percent for different types of pollutants (MacDonald, 2008).

Generally, there are two approaches to implement VSL in freeway facilities: reactive and proactive. Reactive methods wait for activation criteria in a downstream bottleneck to activate VSL upstream of it (Malikopoulos et al. 2016, Burgess 2008). Therefore, VSL is activated after congestion detection and there would be a lag to manage the congestion (Khondaker and Kattan, 2015). To address this issue, proactive approaches are presented to predict the onset of congestion in near future and apply appropriate strategies in advance to avoid it (Khondaker and Kattan, 2015).

Several mathematical programs are developed aiming at minimizing travel time, the variance of the speeds, or the density on a specific section of the road via proactive control

strategies (Malikopoulos *et al.*, 2016). Model predictive control is an appropriate approach to implement proactive VSL strategies (Hegyi et al. 2005, Camacho & Bordons 2012, van de Weg et al. 2015). As a result of implementing proactive VSL on freeway facilities, Khondaker & Kattan (2015) showed 20%, 11%, and 16% improvements in total travel time, time to collision, and fuel consumption, respectively assuming a fleet of 100% connected vehicles. Furthermore, Grumert et al. (2015) considered VSL to assign speeds to CAVs based on their distance to possible incident locations on freeway facilities. They showed that speed harmonization was associated with a reduction in emissions.

2.3 Dynamic speed harmonization in arterial streets

Information on the trajectory of approaching vehicles and upcoming signal timing plans is used in recent studies to provide vehicles with optimal advisory speeds that reduce the likelihood of stopping at intersections thus reduce fuel consumption. In addition, providing advanced knowledge of signal phasing and timing (SPaT) information to vehicles has been shown improvement in traffic safety, mobility, and fuel consumption efficiency (Asadi and Vahidi, 2010; He, Liu and Liu, 2015; HomChaudhuri, Vahidi and Pisu, 2015). Based on a report by the national highway traffic safety administration (NHTSA), SPaT broadcasts will help reduce red-light violations and energy consumption by 90% and 35%, respectively (Misener, Shladover and Dickey, 2010). Decreasing fuel consumption was the primary objective of DSH systems in arterial streets (Kamalanathsharma et al. 2015, Wan et al. 2016, Xia et al. 2013). Vehicle trajectories can be planned to reduce stops at intersections and minimizing fuel consumption. Xia et al. (2012) showed that a 14% reduction in fuel consumption is possible as a result of an advisory speed system experiment at a fixed-time signalized intersection.

DSH systems can provide advisory speeds to individual vehicles (Almqvist, Hydén and Risser, 1991) or the platoon leader (Sanchez, Cano and Kim, 2006), where second ordered traffic flow models could be used to find the optimal acceleration and deceleration rates corresponding to each vehicle in the network (Mandava, Boriboonsomsin and Barth, 2009). Wei et al. (2017) illustrated that controlling the speed of leading vehicle in a platoon would be enough to effectively manage the traffic congestion and increase the capacity in a network. Wan et al. (2016) showed that speed harmonization not only reduces the fuel consumption of CAVs, but also controls the motion of non-equipped vehicles in a mixed environment and contributes to more energy savings on the roads. He et al. (2015) considered the constraints of queue formation at intersections to prevent infeasible solutions. This strategy helped reduce fuel consumption by 29% while travel time was increased by 9%.

2.4 Dynamic speed harmonization in urban networks

Wang (2013) investigated the impact of harmonized speeds on transportation networks from a macroscopic perspective in combination with static traffic assignment. A bi-level formulation is used, where the upper level finds the best speed limit for predefined links, and based on that, the lower level solves static user equilibrium traffic assignment. The solutions found by this approach did not necessarily yield a reduction in travel time.

Moreover, Yan et al. (2015) considered a traffic assignment problem in a network with a stochastic travel time function and a degradable link capacity. Based on this study, a function is provided to activate a speed limit on a link based on its actual capacity. This study showed that reducing the speed limit leads to a reduction in the variance of speed over the network. However, the average speed may increase or decrease. Yang et al. (2013) investigated finding optimal

speed limits on network links using a three-objective bi-level programming. In the first level, the speed limit is found by solving a user equilibrium traffic assignment problem and the second level takes care of system travel time, estimated number of accidents, and traffic emissions. All mentioned studies included a static traffic assignment component, as such, they cannot consider traffic flow dynamics that exists in real-world transportation networks.

Zhu & Ukkusuri (2014) studied dynamic speed limit control in a connected vehicle environment. They considered a trade-off between the travel time and emissions to find the optimal speed at each link of the transportation network. Markov Decision processes were used to find the speed limit at each link and at each time step. This study reduced the total travel time and emissions by 18% and 20%, respectively compared to not controlling the speed limits dynamically.

2.5 Coordinated signal timing and speed harmonization

In addition to optimizing vehicle speeds in transportation network based on fixed signal timing, some studies considered optimizing both signal timing and vehicles' speed cooperatively. For instance, Hao et al. (2015) considered an eco-driving strategy to be applied on an actuated signalized intersection by taking into account the minimum and maximum times to the next phase. The simulation results showed a significant reduction in fuel consumption by 12%. Li et al. (2014) optimized signal timing plans in cooperation with vehicle trajectories in a single intersection with two phases. Their results showed the average travel delay reduction by 16.2% - 36.9% and a throughput increase by 2.7% - 20.2% in comparison with an actuated signal control. Jung et al. (2016) applied an eco-traffic signal system in an isolated intersection using bi-level programming and showed a 5% - 10% reduction in fuel consumption and up to 12% reduction in travel time compared to exiting signal control strategies. Similarly, Xu et al. (2018) utilized a bi-level programming method incorporated in a receding horizon technique to optimize traffic signal timing and vehicle trajectories at an isolated intersection. Testing the proposed approach in Vissim showed reductions in fuel consumption, total travel time, and the number of stops in comparison with actuated signal timing, and independent vehicle speed control. Kaths (2016) developed a single-level optimization program for joint signal and speed optimization and simulated the proposed model in SUMO for a single intersection. The results showed that cooperative signal and speed optimization was able to reduce the number of stops and delay by 36.3% and 56.2%, respectively compared to only signal timing optimization. In contrast with other studies that focused on a single intersection network, Li et al. (2018) added signal timing optimization to the eco-driving problem of electric vehicles in a four-intersection arterial street. They showed that there exists a trade-off between delay and energy saving of electric vehicles. Particularly, they showed that changing the objective function weights from only signal optimization to both signal and energy optimization could yield to a 14% delay increase, while an 11% energy consumption reduction was achieved in over-congested traffic condition.

2.6 Strategies to reduce the computational complexity of traffic control problems

Harmonizing the speed of vehicles in large urban street networks is computationally complex and requires strategies that reduce the complexity of the problem. In general, decentralization, decomposition, and distribution methods are used for this purpose. More explanations follow:

2.6.1 Decomposition approaches for traffic control

Decomposition approaches have been used widely to solve complex transportation engineering problems (Hajibabai and Ouyang, 2013; Hajibabai and Saha, 2019; Mehrabipour, Hajibabai and Hajbabaie, 2019; Amir Mirheli and Hajibabai, 2020). Tettamanti & Varga (2010) integrated this approach in MPC to optimize signal timing parameters by minimizing queue length at intersections. They iteratively solved the problem and determined the Lagrangian multipliers to find near-optimal signal timing plans. Testing the proposed methodology in a network of four intersections resulted in reducing the travel time by 13% compared to optimized fixed-time signal control. Papageorgiou and Mayr (1982) also developed a ramp metering problem and solved it using the Lagrangian decomposition technique. They reduced the problem complexity by decomposing the roadway into different segments and computed the Lagrangian multipliers for each segment iteratively.

To improve the convergence of the Lagrangian relaxation technique, the Alternating Direction Method of Multiplier (ADMM) approach is introduced (Boyd *et al.*, 2011). Timotheou et al. (2015) used ADMM and solved the signal timing optimization problem by decomposing the network of four intersections and achieved solutions with an 8% optimality gap.

2.6.2 Distributed Optimization and Coordination Algorithms (DOCA) for traffic control

Most of the reviewed studies developed problem decomposition solution techniques, but still, need a central controller to find the solution for each subproblem and coordinate them. The advancement of connected and automated technologies enables utilizing distributed techniques, where a controller could be assigned to each subproblem without the presence of a central controller. As a result, the controllers can communicate with each other and share the required information through a communication environment and find near-optimal solutions. For instance, Araghi et al. (2015) utilized the distributed control algorithm to solve the signal timing optimization problem in a network. They decomposed the network into several intersections and solve each subproblem by minimizing traffic delay using the Q-learning concept. Their proposed algorithm let adjacent intersections share information about the flow of incoming vehicles and as a result, reduced average delay by more than 35% compared to predetermined signal timing plans. Similarly, Islam and Hajbabaie (2017) proposed a distributed optimization and coordination algorithm to find optimal signal timing plans in a connected network. As a result of their algorithm, the network travel time was reduced between 17% and 48%, and solutions were found in real-tome Mehrabipour and Hajbabaie (2017) also developed a real-time and scalable distributed-coordinated methodology for signal timing optimization with a maximum of 2% optimality gap.

2.7 Summary

The review of the literature indicates that most network-level speed harmonization problems are formulated with static traffic models. Therefore, they do not consider dynamic traffic changes in the network. Besides, they are not scalable with the size of the transportation network and cannot find optimal solutions in real-time. As a result, they might not be suitable for real-world applications.

Moreover, joint signal timing and speed optimization was not studied in large scale networks due to its high computational complexities. Although decomposition techniques were able to reduce the problem complexity, they generally could not provide near-optimal solutions. In addition, their application to real-world problems was limited due to their slow convergence.

Chapter 3. Problem Formulation

3.1 Introduction

This section presents two formulations for speed harmonization in urban street networks. In the first formulation, advisory speeds are dynamically optimized on each network link while signal timing parameters are predetermined and input to the optimization program. The second formulation optimizes advisory speeds and signal timing parameters cooperatively. Both formulations are based on the cell transmission model (CTM) (Daganzo, 1994), where the time is discretized into short intervals and each network link is represented by several cells. Discretizing the time will reduce the computational burden in capturing the dynamic nature of the problem as opposed to using a continuous time (Hajibabai and Ouyang, 2016; A Mirheli and Hajibabai, 2020). The length of the cells must be equal to the distance traveled in free-flow conditions in one time-step. We define C, C_R, C_S, and C_I as the sets of all, source, sink, and intersection cells, respectively. Set T represents all discrete time steps. In addition, set Γ_i indicates all cell successor to cell $i \in C$, and Γ_i^{-1} represents all cells predecessor to cell $i \in C$. In CTM, the occupancy of cell $i \in C$ at time $t \in T$ is defined by the decision variable x_i^t. Furthermore, flow from cell $i \in C$ to subsequent cell $j \in \Gamma_i$ is determined by the decision variable y_{ij}^t. Variable v_i^t represents the space mean speed in cell $i \in C$ at time step $t \in T$. Table 3-1 provides a summary of notations used in this study

3.2 Speed harmonization problem

The objective function of the optimization program minimizes the difference between space mean speeds in a cell in two subsequent time steps and the differences between space mean speeds in two subsequent cells at the same time. In addition, the cumulative number of completed trips is maximized as suggested by prior research (Medina, Hajbabaie and Benekohal, 2010, 2011; Hajbabaie and Benekohal, 2013, 2015). Equation (3-1) indicates the objective function. We define parameter γ (vehicle/mph) as factor to give a desired weight on the second term of the objective function.

$$\boldsymbol{Max}\left[\sum_{t\in T}\sum_{i\in C_S} x_i^t - \gamma \sum_{t\in T}\sum_{i\in C\setminus\{C_S\}}\sum_{j\in\{i,\Gamma_i\}}\left|v_i^t - v_j^{t+1}\right|\right] \tag{3-1}$$

Table 3.1: Summary of notations

Sets	Description
C	set of all cells
C_R	set of all source cells
C_S	set of all sink cells
C_I	set of all intersection cells
Γ_i	set of all successors of cell $i \in C$
Γ_i^{-1}	set of all predecessors of cell $i \in C$
T	set of all time intervals
Variables	
x_i^t	number of vehicles in cell $i \in C$ at time step $t \in T$
y_{ij}^t	number of vehicles moving from cell $i \in C$ to cell $j \in \Gamma_i$ at time step $t \in T$

v_i^t	space mean speed in cell $i \in C$ at time step $t \in T$
z_{ii}^t	auxiliary variable
u_{ii}^t	auxiliary variable
Parameters	
N_i	jam density of cell $i \in C$
Q_i^t	outflow capacity of cell $i \in C$ at time step $t \in T$
D_r^t	demand from source cell $r \in C_R$ at time step $t \in T$
f_i^t	green time indicator for signals at cell $i \in C_I$ at time step $t \in T$
v_f	free flow speed
w	shock wave speed
β_i	turning percentage at intersection cell $i \in C_I$
k_j	jam density
q_{max}	maximum flow
γ	weight factor
α	weight factor
θ	the angle between speed vectors
Indices	
i	index for cells
j	index for cells
u	index for cells
p	index for cells
k	index for cells
t	index for time intervals
r	index for source cells
s	index for sink cells

The fundamental diagram of traffic flow in the cell transmission model is a trapezoid (Daganzo, 1994). Figure 3-1 shows the flow-density relationship in the cell transmission model. In this figure, k_j is the jam density and q_{max} is the maximum flow, which is always less than or equal to $\frac{wv_f k_j}{w+v_f}$. As fundamental relationship of traffic flow suggests, the average space mean speed could be found based on equation (3-2). Considering Δt as a time step and Δx as the length of a cell, the free flow speed v_f is equal to the ratio of $\frac{\Delta x}{\Delta t}$ in the cell transmission model. Thus, the space mean speed in cell $i \in C$ at time $t \in T$ would be estimated based on equation (3-3) (Zhu and Ukkusuri, 2014).

$$\boldsymbol{v_i^t = \frac{q_i^t}{k_i^t} = \frac{\sum_{j\in\Gamma_i} y_{ij}^t/\Delta t}{x_i^t/\Delta x} = \frac{\sum_{j\in\Gamma_i} y_{ij}^t}{x_i^t}\frac{\Delta x}{\Delta t}} \tag{3-2}$$

$$\boldsymbol{v_i^t = \begin{cases} \frac{\sum_{j\in\Gamma_i} y_{ij}^t}{x_i^t} v_f & x_i^t > 0 \\ v_f & x_i^t = 0 \end{cases} \qquad \forall\, i \in C, t \in T} \tag{3-3}$$

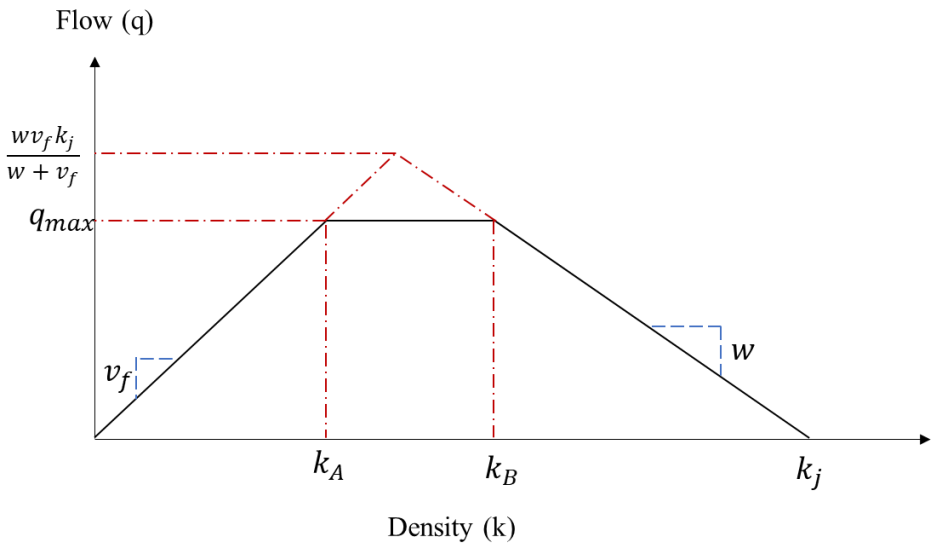

Figure 3.1: **Fundamental diagram of traffic flow in CTM.**

Constraints (3-4) show the flow conservation constraints for different cells in the network. The Kronecker delta δ_{ij} takes the value of 1 when $i = j$ and zero, otherwise. Based on equations (3-4), the number of vehicles x_i^{t+1} in cell i at time step $t+1$ is equal to the number of vehicles x_i^t in that cell, plus the flow entered from all upstream cells $u \in \Gamma_i^{-1}$, minus the outflow left to all downstream cells $j \in \Gamma_i$ at time step t.

$$(\delta_{il} + \delta_{is}) \sum_{u \in \Gamma_i^{-1}} y_{ui}^t - (\delta_{ir} + \delta_{il}) \sum_{j \in \Gamma_i} y_{ij}^t + D_i^t(\delta_{ir}) = (\delta_{il} + \delta_{ir} + \delta_{is})(x_i^{t+1} - x_i^t) \qquad \forall i \in C, \forall l \in C \ \{C_S, C_R\}, \forall r \in C_R, \ \forall s \in C_S, t \in T \tag{3-4}$$

The flow between two subsequent cells is constrained by cell occupancy at the upstream cell, saturation flow rates, signal status at intersection cells, and available room to receive vehicles at the downstream cell. Constraints (3-5) to (3-9) indicate these limitations. The turning ratios at intersection cells are predefined and are equal to β_j at cell $j \in C_I$. These constraints are provided in (3-10). Finally, Constraints (3-11) and (3-12) ensure that the decision variables are non-negative.

$$\sum_{j \in \Gamma_i} y_{ij}^t \leq x_i^t \qquad \forall \, i \in C \backslash C_S, t \in T \tag{3-5}$$

$$\sum_{j \in \Gamma_i} y_{ij}^t \leq Q_i^t \qquad \forall \, i \in C \backslash C_S, t \in T \tag{3-6}$$

$$\sum_{i \in \Gamma_j^{-1}} y_{ij}^t \leq Q_j^t \qquad \forall \, j \in C \backslash C_R, t \in T \tag{3-7}$$

$$\sum_{j\in\Gamma_i} y_{ij}^t \le f_i^t Q_i^t \qquad \forall\, i \in C_I, t \in T \qquad (3\text{-}8)$$

$$\sum_{i\in\Gamma_j^{-1}} y_{ij}^t \le \frac{w}{v_f}\left(N_j - x_j^t\right) \qquad \forall\, j \in C\backslash C_R, t \in T \qquad (3\text{-}9)$$

$$y_{ij}^t = \beta_j^t \sum_{k\in\Gamma_i} y_{ik}^t \qquad \forall\, j \in C_I, i \in \Gamma_j^{-1}, t \in T \qquad (3\text{-}10)$$

$$x_i^t \ge 0 \qquad \forall\, i \in C, t \in T \qquad (3\text{-}11)$$

$$y_{ij}^t \ge 0 \qquad \forall\, i \in C\backslash C_S, j \in \Gamma_i, t \in T \qquad (3\text{-}12)$$

3.3 Linear speed control

As shown in DSH problem formulation, all constraints are linear and there is no integer variable in the problem. However, the fraction terms (space mean speed is the fraction of flow to occupancy) the absolute value functions in the second term of the objective function make the formulation nonlinear and nonconvex. In addition, the units of different terms in the objective function are not the same. Therefore, the fundamental diagram of traffic flow is used to resolve these issues and reduce the complexity of the problem.

Based on the fundamental diagram of traffic flow, shown in Figure 3-1, space mean speed in cell $i \in C$ at time $t \in T$ can be measured as the slope of a vector that connects the origin to point x_i^t and y_{ij}^t on the fundamental diagram. It is assumed that space mean speed in subsequent cell $j \in \Gamma_i$ at time $t+1 \in T$ is equal to the slope of a vector that connects the origin to point x_j^{t+1} and y_{jk}^{t+1} when $k \in \Gamma_j$. Figure 3-2 shows these vectors. Minimizing the difference of two speed vectors is equivalent to minimizing the angle θ between them. Furthermore, minimizing this angle is equivalent to minimizing the difference between the distances of points $\left(x_i^t, y_{ij}^t\right)$ and $\left(x_j^{t+1}, y_{jk}^{t+1}\right)$ to the vector that represents free flow speed. The space mean speed in a cell will be equal to free-flow speed when all vehicles in the cell exit in a time step and the outflow is equal to the occupancy of the cell. Equation (3-13) shows this condition. The distance of each point $\left(x_i^t, y_{ij}^t\right)$ to the vector that represents equation (3-13) is equal to $x_i^t - y_{ij}^t$. Therefore, the objective function (3-1) can be presented as (3-14). Note that both terms of objective function (3-14) contain the same units. Therefore, we replace parameter γ with unit-less term α.

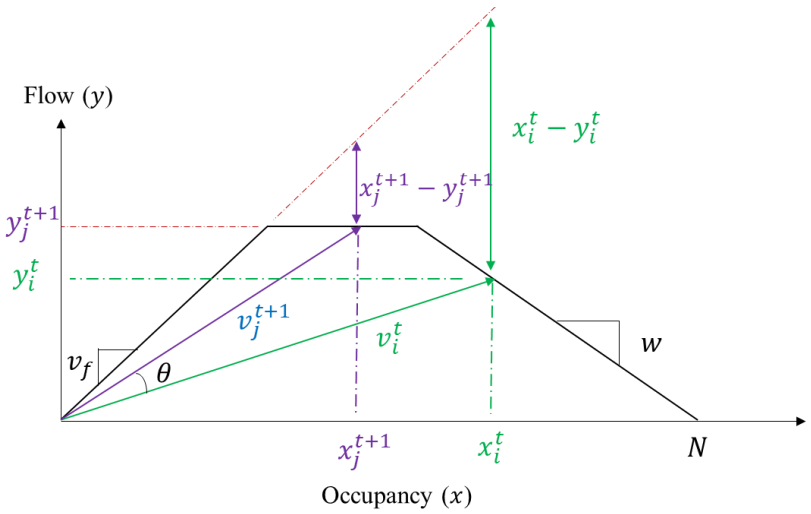

Figure 3.2: **Linearizing speed differences using traffic flow fundamental diagram**

$$\frac{\sum_{p\in\Gamma_i} y_{ip}^t}{x_i^t} = 1 \qquad \forall\, i \in C, t \in T \tag{3-13}$$

$$\alpha \sum_{t\in T}\sum_{i\in C_S} x_i^t - (1-\alpha)\sum_{t\in T}\sum_{i\in C\setminus C_s}\sum_{j\in\{i,\Gamma_i\}}\left|\left(x_i^t - \sum_{p\in\,\Gamma_i} y_{ip}^t\right) - \left(x_j^{t+1} - \sum_{k\in\,\Gamma_j} y_{jk}^{t+1}\right)\right| \tag{3-14}$$

As mentioned, the absolute value function in the new objective function is still nonlinear. To linearize it, two auxiliary variables z_{ij}^t and u_{ij}^{t+1} are introduced. Using these two variables, the objective function can be rewritten as equation (3-15). Besides, constraints (3-16) - (3-18) are added to the problem. With these transformations, the nonlinear optimization program is converted to a linear program.

$$\alpha \sum_{t\in T}\sum_{i\in C_S} x_i^t - (1-\alpha)\sum_{t\in T}\sum_{i\in C\setminus C_s}\sum_{j\in\{i,\Gamma_i\}}\left(z_{ij}^t + u_{ij}^{t+1}\right) \tag{3-15}$$

$$z_{ij}^t - u_{ij}^{t+1} = \left(x_i^t - \sum_{p\in\,\Gamma_i} y_{ip}^t\right) - \left(x_j^{t+1} - \sum_{k\in\,\Gamma_j} y_{jk}^{t+1}\right) \qquad \forall\, i \in C\setminus C_S, j \in \{i,\,\Gamma_i\}, t \in T \tag{3-16}$$

$$z_{ij}^t \geq 0 \qquad \forall\, i \in C\setminus C_S, j \in \{i,\,\Gamma_i\}, t \in T \tag{3-17}$$

$$u_{ij}^t \geq 0 \qquad \forall\, i \in C\setminus C_S, j \in \{i,\,\Gamma_i\}, t \in T \tag{3-18}$$

3.4 Cooperative signal timing and speed harmonization

Traffic operations can be further improved by jointly optimizing signal timing parameters and advisory speeds. In this section, we present a mathematical program for Coordinated Signal timing and Speed Harmonization (CSSH) in connected urban-street networks, where intersection controllers are connected to each other and to vehicles in the network.

Signal controllers at each intersection are in charge of finding the optimal green time duration and phase sequence in addition to optimizing the advisory speeds on intersection links. The speed harmonization formulation presented earlier in this chapter is enhanced by adding new constraints and decision variables to optimize signal timing parameters as well. Let the binary variable g_i^t take on the value of one when the signal is green and zero, otherwise. We use constraints (3-19) to change the saturation flow rate (f_i^t) in an intersection cell depending on the status of the upstream signal. At the same time, constraints (3-20) adjust the flow rate (f_i^t) of intersections based on the updated saturation flow rate.

$$f_i^t = g_i^t Q_i^t \qquad \forall\, i \in C_I, t \in T \qquad (3\text{-}19)$$

$$\sum_{j \in \Gamma_i} y_{ij}^t \le f_i^t \qquad \forall\, i \in C_I, t \in T \qquad (3\text{-}20)$$

We define parameter f' as the saturation flow reduction rate to take into account the start-up lost time. We reduce the saturation flow rate of the intersection at the initiation of green time using constraints (3-21).

$$\sum_{j \in \Gamma_i} y_{ij}^{t+1} \le Q_i^t - Q_i^t f'\left(g_i^{t+1} - g_i^t\right) \qquad \forall\, i \in C_I,\ t \in T \qquad (3\text{-}21)$$

We prevent the possibility of a collision between two conflicting movements $(i,j) \in C_F$, where C_F is the set of all conflicting movements at an intersection. Based on Constraints (3-22), only one of the two conflicting movements $(i,j) \in C_F$ gets the green time at a time.

$$g_i^t + g_j^t \le 1, \qquad \forall\, (i,j) \in C_F, t \in T \qquad (3\text{-}22)$$

The green duration for each approach of the intersection is limited between a minimum green time G_{min}^i and a maximum green time G_{max}^i by Constraints (3-23) and (3-24), respectively.

$$\sum_{j=t}^{t+G_{max}^i+1} g_j^t \le G_{max}^i, \qquad \forall\, i \in C_I, t < T - G_{max}^i \qquad (3\text{-}23)$$

$$\sum_{j=t+1}^{t+G_{min}^i} g_j^t \ge \left(g_i^{t+1} - g_i^t\right) G_{min}^i, \qquad \forall\, i \in C_I, t \le T - G_{min}^i \qquad (3\text{-}24)$$

The set C_{RT} is defined as the set of concurrent adjacent right and through movements. This set is used in constraints (3-25) to make sure that adjacent right turn and through movements receive the same signal plan.

$$g_i^t = g_j^t, \qquad \forall\, (i,j) \in C_{RT}, t \in T \qquad (3\text{-}25)$$

Chapter 4. Real-Time Solutions for Dynamic Speed Harmonization Problem Introduction

4.1 Introduction

In this chapter, we use distributed optimization techniques to optimize the advisory speeds of CAVs in real-time. The proposed problem formulation for the speed harmonization problem, with or without signal timing cooperation, is not scalable to different network sizes or long study periods due to an excessive number of continuous and integer decision variables. Hence, developing Distributed Optimization and Coordination Algorithms for Dynamic Speed Harmonization (DOCA-DSH) provides an opportunity for finding real-time and near-optimal solutions in large-scale urban street networks. Distributed optimization decomposes the network-level problem into several subnetwork-level subproblems to reduce the problem complexity. Distributed coordination among different subnetworks helps push local solutions toward the global optimal solution. We also utilize model predictive control (MPC) to provide a consensus between subproblems and take into account the dynamic fluctuations in traffic demand and capacity.

4.2 Distributed optimization

To reduce the computational complexity of the problem, Distributed optimization decomposes the network into smaller subnetworks. Decomposing the network into intersection-level subnetworks let the intersection controllers adjust the speed limits on the upstream and downstream cells in addition to signal timing parameters at each intersection (Islam et al., 2020; Islam and Hajbabaie, 2017; Mehrabipour and Hajbabaie, 2017). In this decomposition, the links that connect two intersections are broken and the dummy source and sink cells are added to each segment. Figure 4-1.a shows a two-intersection network, where the links connecting cell 7 to 8 and cell 21 to 22 are cut. Therefore, the network is divided into intersections 1 and 2. This breaking is equivalent to relaxing the following constraints:

$$x_i^{t+1} = x_i^t + \sum_{u \in \Gamma_i^{-1}} y_{ui}^t - \sum_{j \in \Gamma_i} y_{ij}^t \qquad \forall\, i \in \{7,8,21,22\}, t \in T \qquad (4\text{-}1)$$

$$\sum_{j \in \Gamma_i} y_{ij}^t \le Q_i \qquad \forall\, i \in \{7,21\}, t \in T \qquad (4\text{-}2)$$

$$\sum_{i \in \Gamma_j^{-1}} y_{ij}^t \le Q_j \qquad \forall\, j \in \{8,22\}, t \in T \qquad (4\text{-}3)$$

$$\sum_{i \in \Gamma_j^{-1}} y_{ij}^t \le \frac{W}{v_f}\left(N_j - x_j^t\right) \qquad \forall\, j \in \{8,22\}, t \in T \qquad (4\text{-}4)$$

$$z_{ij}^t - u_{ij}^{t+1} = \left(x_i^t - \sum_{p \in \Gamma_i} y_{ip}^t\right) - \left(x_j^{t+1} - \sum_{k \in \Gamma_j} y_{jk}^{t+1}\right) \qquad \forall\, i \in \{6,7,20,21\},\ j \in \{7,8,21,22\}, t \in \mathrm{T} \qquad (4\text{-}5)$$

Figure 4-1.b shows the two intersections after adding dummy source and sink cells. Dummy source and sink cells 22’ and 8’’ were added to intersection 1, respectively. Similarly, dummy source and sink cells 8’ and 22’’ were added to intersection 2.

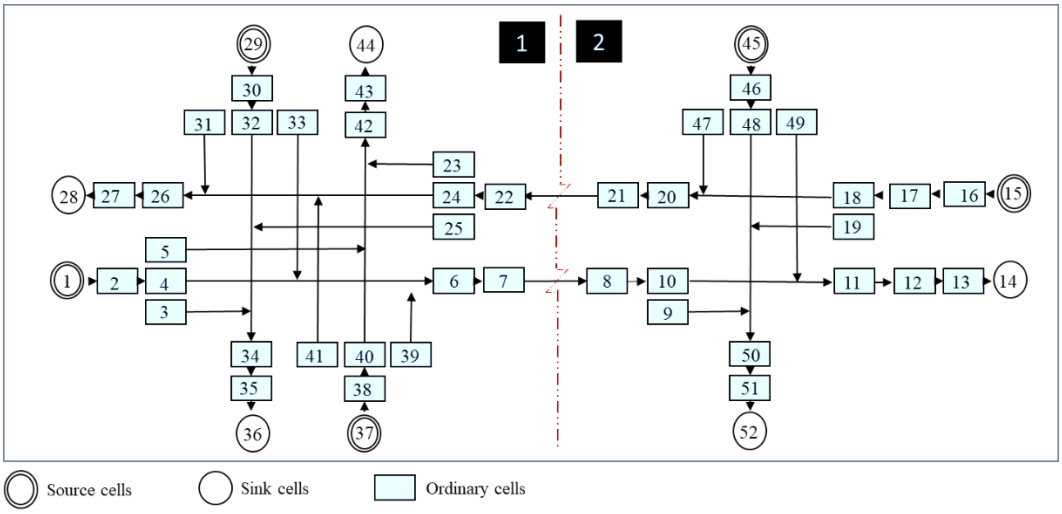

a) before decomposition

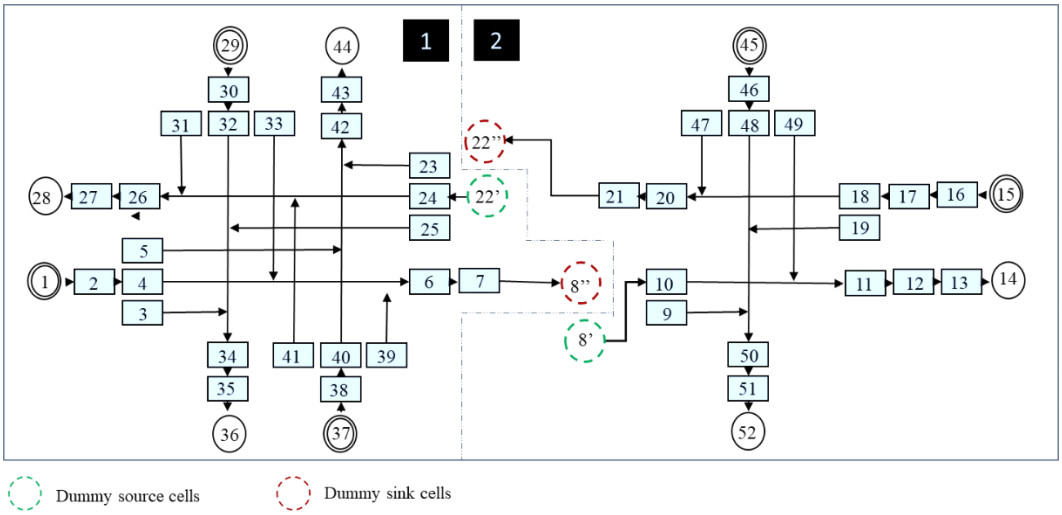

b) after decomposition

Figure 4.1: **Decomposition of two-intersection network**

To formulate the subproblems, we define S as the set of all intersections. Furthermore, sets C_{SD}^{n} and C_{RD}^{n} are introduced as the set of all dummy source and dummy sink cells, respectively at intersection $n \in S$. After the decomposition, the original problem is presented as the following LP for each intersection $n \in S$:

$$\text{Max}\left[\alpha\sum_{t\in T}\sum_{i\in\{C_S^n\cup C_{SD}^n\}}x_i^t-(1-\alpha)\sum_{t\in T}\sum_{i\in C\backslash\{C_S^n\cup C_{SD}^n\}}\sum_{j\in\{i,\,\Gamma_i\}}\left(z_{ij}^t+u_{ij}^{t+1}\right)\right] \tag{4-6}$$

s.t.

$$x_r^{t+1}=D_r^t+x_r^t-\sum_{j\in\Gamma_i}y_{rj}^t \qquad \forall\, r\in\{C_R^n\cup C_{RD}^n\},t\in T \tag{4-7}$$

$$x_s^{t+1}=x_s^t+\sum_{i\in\Gamma_s^{-1}}y_{is}^t \qquad \forall\, s\in\{C_S^n\cup C_{SD}^n\},t\in\ T \tag{4-8}$$

$$x_i^{t+1}=x_i^t+\sum_{u\in\Gamma_i^{-1}}y_{ui}^t-\sum_{j\in\Gamma_i}y_{ij}^t \qquad \forall\, i\in C^n\backslash\{C_S^n\cup C_{SD}^n\cup C_R^n\cup C_{RD}^n\},t\in T \tag{4-9}$$

$$\sum_{j\in\Gamma_i}y_{ij}^t\le x_i^t \qquad \forall\, i\in C^n\backslash\{C_S^n\cup C_{SD}^n\},t\in T \tag{4-10}$$

$$\sum_{j\in\Gamma_i}y_{ij}^t\le Q_i \qquad \forall\, i\in C^n\backslash\{C_S^n\cup C_{SD}^n\},t\in T \tag{4-11}$$

$$\sum_{i\in\Gamma_j^{-1}}y_{ij}^t\le Q_j \qquad \forall\, j\in C^n\backslash\{C_R^n\cup C_{RD}^n\},t\in T \tag{4-12}$$

$$\sum_{i\in\Gamma_j^{-1}}y_{ij}^t\le\frac{\mathrm{W}}{v_f}\left(N_j-x_j^t\right) \qquad \forall\, j\in C^n\backslash\{C_R^n\cup C_{RD}^n\},t\in T \tag{4-13}$$

$$\sum_{j\in\Gamma_i}y_{ij}^t\le f_iQ_i \qquad \forall\, i\in C_I^n,t\in T \tag{4-14}$$

$$y_{ij}^t=\beta_j\sum_{k\in\Gamma_i}y_{ik}^t \qquad \forall\, j\in C_I^n,i\in\Gamma_j^{-1},t\in T \tag{4-15}$$

$$z_{ij}^t-u_{ij}^{t+1}=\left(x_i^t-\sum_{p\in\ \Gamma_i}y_{ip}^t\right)-\left(x_j^{t+1}-\sum_{k\in\ \Gamma_j}y_{jk}^{t+1}\right) \qquad \forall\, i\in C^n\backslash\{C_S^n\cup C_{SD}^n\},\ j\in\{i,\,\Gamma_i\},t\in T \tag{4-16}$$

$$z_{ij}^t\ge 0 \qquad \forall\, i\in C^n\backslash\{C_S^n\cup C_{SD}^n\},j\in\{i,\,\Gamma_i\},t\in T \tag{4-17}$$

$$u_{ij}^t\ge 0 \qquad \forall\, i\in C^n\backslash\{C_S^n\cup C_{SD}^n\},j\in\{i,\,\Gamma_i\},t\in T \tag{4-18}$$

$$x_i^t\ge 0 \qquad \forall\, i\in C^n,t\in T \tag{4-19}$$

$$y_{ij}^t\ge 0 \qquad \forall\, i\in C^n\backslash\{C_S^n\cup C_{SD}^n\},j\in\Gamma_i,t\in T \tag{4-20}$$

It should be noted that the signal timing constraints (3-19)-(3-25) can also be added to each intersection subproblem to find the optimal signal timing plan in addition to the average speed of vehicles around the intersection.

4.3 Distributed coordination

The spatial decomposition of the network lets solve the dynamic speed harmonization problems separately for the corresponding subnetworks. However, solving the DSH problem for a subnetwork will not yield a network-wide optimal solution without considering the condition of the adjacent subnetworks. As a result, the DSH formulation should be modified to include the necessary information from the neighboring segments. Since the connected vehicle environment provides an opportunity for infrastructure to infrastructure communications, the controllers can share the required information. Coordination between neighboring subnetworks can be achieved by sharing the following information:

- The outflow from the upstream subnetwork,
- The available capacity of receiving cell at the downstream subnetwork,
- The average speed of the receiving cell at the downstream subnetwork,
- The signal status at the downstream intersection cell.

To formulate the DSH problem for a decomposed network, S is introduced as the set of all subnetworks in the network. For subnetwork $n \in S$, parameter $D'^{t,n}_r$ is introduced for cell $r \in C_{RD}$, which represents the inflow from the subnetwork upstream of n. Parameter $N'^{t,n}_i$ is also introduced as the available capacity of the receiving cell $i \in C_{SD}$ at subnetwork downstream of n. In addition, $V'^{t,n}_i$ is defined as the difference of the occupancy and outflow $\left(x'^t_j - \sum_k y'^t_{jk}\right)$ at the receiving cell $i \in C_{SD}$ at subnetwork downstream of n. Parameter $f'^{t,n}_i$ represents the status of the signal at the intersection located at downstream of cell $i \in C_{SD}$. When the signal is green, it takes the value one and zero, otherwise. We modified the first term of the objective function (4-21) to maximize the number of completed trips only when the receiving downstream intersections have a green signal, as follows:

$$\alpha\left(\sum_{t\in T}\sum_{i\in C^n_S} x^t_i + \sum_{t\in T}\sum_{i\in C^n_{SD}}\sum_{j\in F_i} \hat{f}^{t,n}_j x^t_i\right) \qquad \forall\, n \in S \quad (4\text{-}21)$$

In the second term of the objective function, the difference of occupancy and outflow at two consecutive cells at two subsequent time steps are minimized. To consider the speed harmonization between two divided subnetworks, the difference of the occupancy and outflow of cell $i \in \Gamma_j^{-1}$ where $j \in C_{SD}$ is minimized with that difference at cell $j \in C_{SD}$ in the upstream subnetwork. Therefore, we added the following term to the objective function of each intersection to take into account the speed difference minimization of cells connected with broken links:

$$\sum_{t\in T}\sum_{j\in C^n_{SD}}\sum_{i\in \Gamma_j^{-1}}\left|\left(x^t_i - \sum_p y^t_{ip}\right) - \left(\hat{x}^t_j - \sum_p \hat{y}^t_{jp}\right)\right| \qquad \forall\, n \in S \quad (4\text{-}22)$$

As a result, equation (4-23) shows the modified objective function of DSH problem considering the above-mentioned changes.

$$Z_n = \text{Max}\Big(\alpha\Big(\sum_{t\in T}\sum_{i\in C_S^n} x_i^t + \sum_{t\in T}\sum_{i\in C_{SD}^n}\sum_{j\in F_i}\hat{f}_j^{t,n}x_i^t\Big) - (1 - \alpha)\Big(\sum_{t\in T}\sum_{i\in C^n\setminus\{C_S^n\cup C_{SD}^n\cup C_{RD}^n\}}\sum_{j\in\{i,\,\Gamma_i\}}\Big|\Big(x_i^t - \sum_p y_{ip}^t\Big) - \Big(x_j^{t+1} - \sum_k y_{jk}^{t+1}\Big)\Big| + \sum_{t\in T}\sum_{j\in C_{SD}^n}\sum_{i\in\Gamma_j^{-1}}\Big|\Big(x_i^t - \sum_p y_{ip}^t\Big) - \Big(\hat{x}_j^t - \sum_p \hat{y}_{jp}^t\Big)\Big|\Big)\Big) \quad \forall\, n \in S \quad (4\text{-}23)$$

We also add constraints (4-24)-(4-25) to the problem to ensure the conservation of flow at dummy source cells and dummy sink cells, respectively. We define $\widehat{D}_i^{t,n}$ as the entry demand to dummy source cell $i \in C_{RD}^n$ in intersection $n \in S$ at time step $t \in$ T. The demand at dummy source cell is equal to the flow $\hat{y}_{ui}^t$ where $u \in \Gamma_i^{-1}$ as shown below:

$$\widehat{D}_i^{t,n} = \hat{y}_{ui}^t \qquad \forall\, i \in C_{RD}^n, t \in T, n \in S \quad (4\text{-}24)$$

Moreover, the capacity $\widehat{N}_i^{t,n}$of dummy sink cell $i \in C_{SD}^n$ at intersection $n \in S$ is measured as the available capacity of the downstream cell with respect to the broken links, see equation (4-25).

$$\widehat{N}_i^{t,n} = \frac{w}{v_f}(N_i^t - \hat{x}_i^t) \qquad \forall\, i \in C_{SD}^n, t \in T, n \in S \quad (4\text{-}25)$$

We also add constraints (4-26) to ensure that the outflow of a subnetwork is less than the available capacity of the downstream subnetwork.

$$\sum_{i\in\Gamma_j^{-1}} y_{ij}^t \le \widehat{N}_j^{t,n} \qquad \forall\, j \in C_{SD}^n, t \in T, n \in S \quad (4\text{-}26)$$

We run a Modified CTM (MCTM) simulation to coordinate the solution of all subproblems and predict the information to be shared among all controllers in the network. The MCTM simulation receives the controllers' optimal speeds and finds the coordinated occupancy and flows over the entire network. Changing the average speed in a network is associated with a change in the corresponding flow. Therefore, we adjust the cell outflow to achieve the optimal speed through equations (4-27) to (4-29).

$$y_{ij}^t = \min\Big\{x_i^t, Q_i, Q_j, \frac{w}{v_f}(N_j - x_j^t), \sum_{j\in\Gamma_i}\hat{y}_{ij}^t\Big\}, \qquad \forall i \in C\setminus\{C_s, C_I, C_d\}, j \in \Gamma_i,\ t \in T \quad (4\text{-}27)$$

$$y_{ij}^t = \beta_j \min\left\{x_i^t, Q_i, \frac{Q_j}{\beta_j}, \frac{\frac{w}{v_f}(N_j - x_j^t)}{\beta_j}, \frac{Q_k}{\beta_k}, \frac{\frac{w}{v_f}(N_k - x_k^t)}{\beta_k}, \sum_{j\in\Gamma_i}\hat{y}_{ij}^t\right\}, \quad \forall i \in C_d, j \in \Gamma_i, k \in \Gamma_i, j \ne k, t \in T \quad (4\text{-}28)$$

$$y_{ij}^t = \min\Big\{x_i^t, f_i, Q_j, \frac{w}{v_f}(N_j - x_j^t), \sum_{j\in\Gamma_i}\hat{y}_{ij}^t\Big\}, \qquad \forall i \in C_I, j \in \Gamma_i, t \in T \quad (4\text{-}29)$$

Finding the adjusted link flows allows finding the optimal occupancies using the flow conservation equalities (3-4). Therefore, the parameters regarding the outflow and the available capacity are extracted from the simulation results and will be transferred to the corresponding subnetwork controller.

4.4 DOCA-DSH framework

To account for unforeseen changes in traffic conditions and reduce the problem complexity, we integrated the DOCA-DSH in a model predictive control framework, where the problem is solved repeatedly over a prediction horizon τ. Then, the solution for the first time step is applied to the system and the time horizon will be rolled forward for one time step. We continue the process until the study period is finished. The general framework for DOCA-DSH approach is shown in Figure 4-2. We solve the DSH problem for each subnetwork over a prediction horizon. Then, the controller at each subnetwork will find the optimal speeds of approaching CAVs and share them with the MCTM simulator. MCTM finds feasible flows in the system and shares the required information with subnetworks. Again each subproblem will be solved.

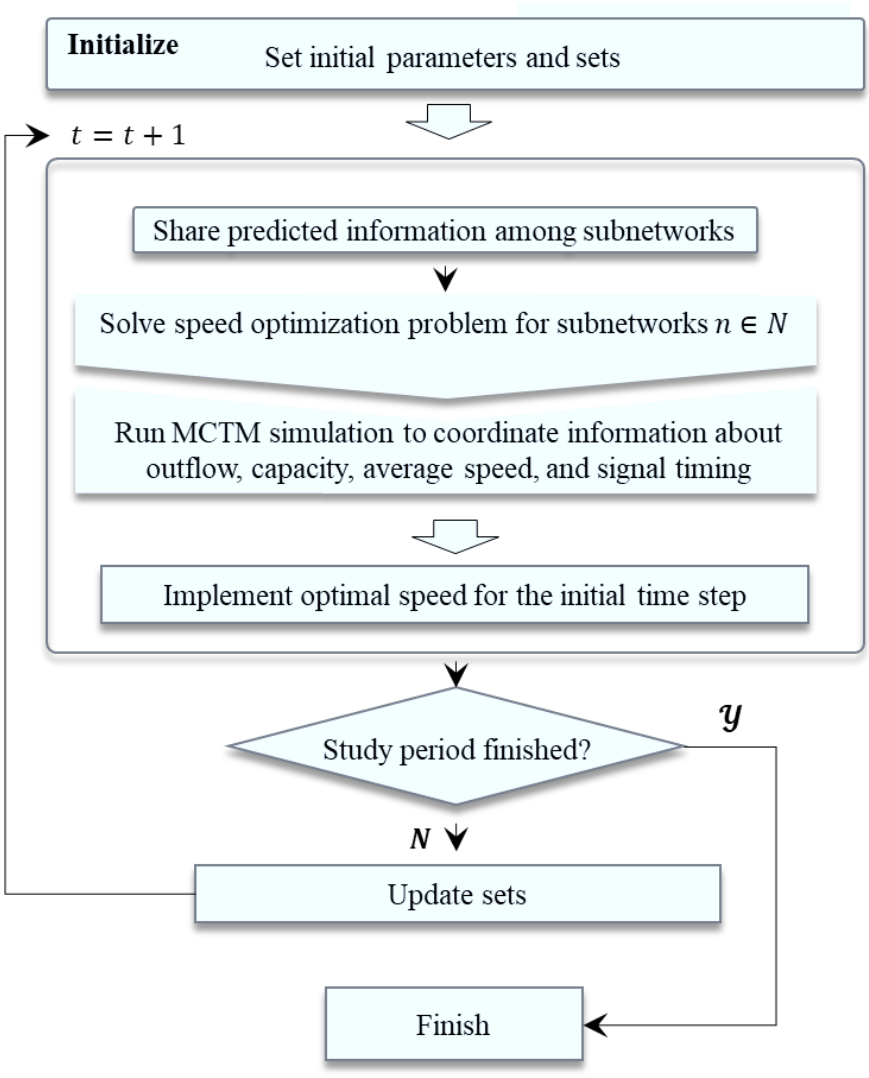

Figure 4.2: **Information flow in Distributed Optimization and Coordination**

Chapter 5. Case Study and Numerical Results

5.1 Case study network

We analyzed three example networks with eight (4 × 2), twenty (4 × 5), and forty (8 × 5) intersections to show the effects of dynamic speed harmonization on traffic operations transportation networks. We considered a portion of downtown Springfield, Illinois as the main case study network to evaluate the proposed dynamic speed harmonization methodologies. The Springfield network is shown in Figure 5-1, where there are 20 intersections with a combination of one-way and two-way streets. Table 5-1 shows the general characteristics of this network. Four different demand patterns were considered as flow:

- Undersaturated symmetric (500 veh/hr/ln),
- Saturated symmetric (900 veh/hr/ln),
- Oversaturated symmetric (1200 veh/hr/ln), and
- Asymmetric dynamic demand pattern, see Figure 5-2.

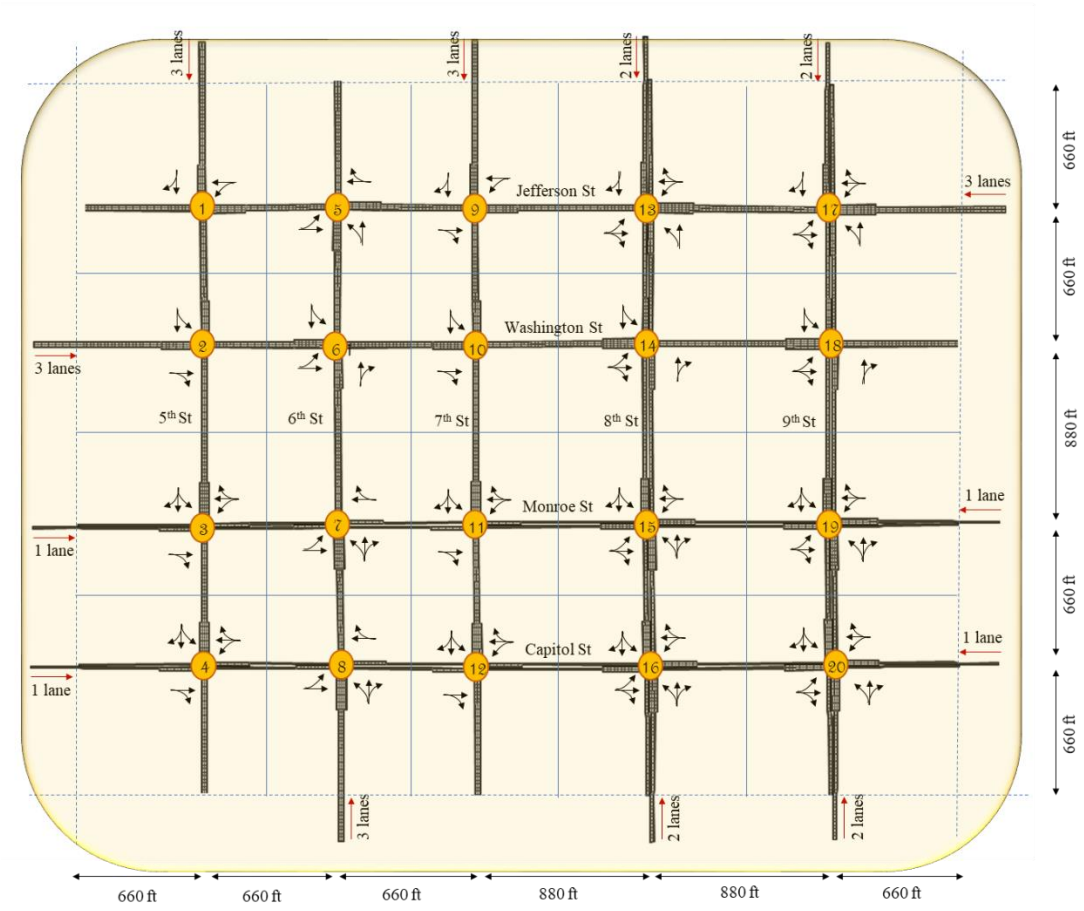

Figure 5.1: **Downtown Springfield, Illinois that is used as the case study network**

Table 5.1: Characteristics of Springfield network in CTM

Link data	
Number of lanes per link	1, 2, or 3
Maximum free-flow speed (mph)	30
Link saturation flow (veh/hour/lane)	1800
Optimization period (time steps)	500
Prediction period (time steps)	15
Duration of each time step (seconds)	6
Number of cells	342
Cell jam density (veh/cell/lane)	12
Cell saturation flow (veh/cell/ lane)	3
Signal timing parameters	
Maximum green for through (seconds)	60
Minimum Green time for through (seconds)	18
Maximum green for left turn (seconds)	24
Minimum green for left turn (seconds)	6

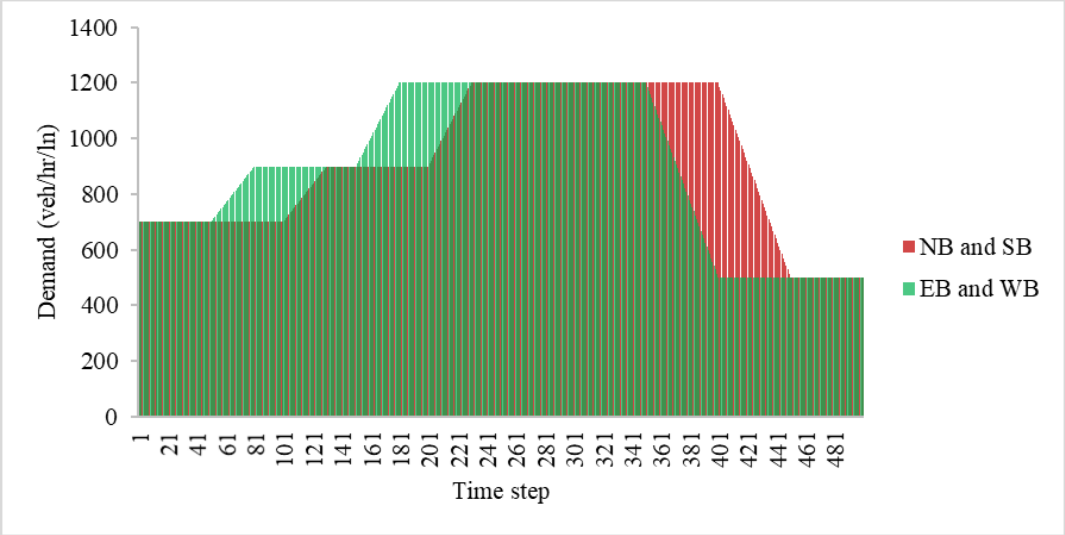

Figure 5.2: **Time-variant demand profile**

5.2 Implementation of the algorithm in Vissim

We used Vissim (PTV Group, 2013) to implement the proposed speed harmonization technique in a simulated environment. Figure 5-3 shows the general implementation procedure. The Component Object Model (COM) interface is utilized to establish communication between vehicles and signal controllers. Particularly, vehicles' location and speed data are passed to DOCA via the COM interface. Then the DSH optimization is solved, and optimal signal timing and speed variables are sent back to Vissim to be implemented in the simulated network.

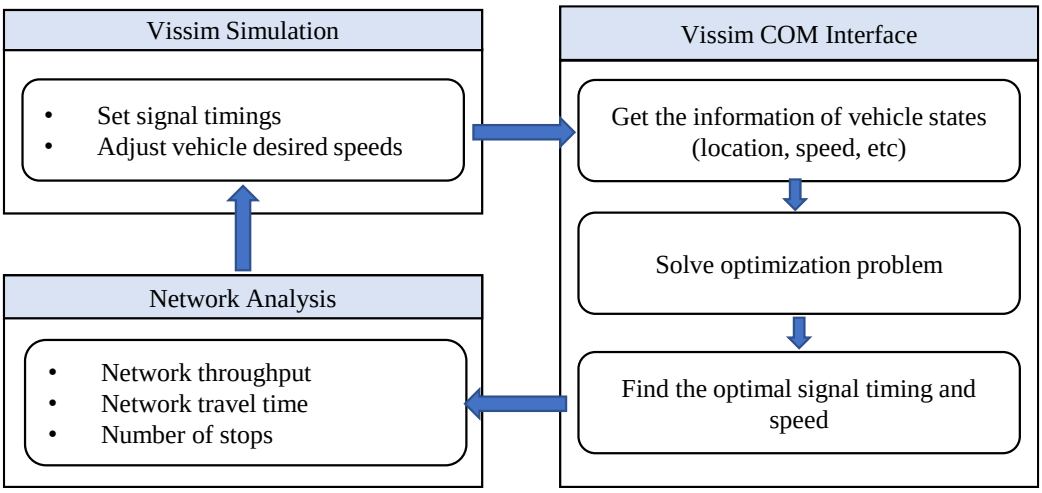

Figure 5.3: **Vissim COM interface to apply the optimized signal timings and speeds**

5.3 Analysis scenarios

The penetration rate of connected and automated vehicles is assumed to be 100%. The following scenarios are considered:

1. No Speed Harmonization: This scenario shows the network performance without providing advisory speeds to vehicles.
2. Dynamic Speed Harmonization (DSH): We used the proposed speed harmonization technique in Chapter 3 to find the optimal advisory speed. This scenario shows the network performance once the optimal speeds are found centrally over the entire analysis period.
3. Distributed Optimization and Coordinated Algorithms for Dynamic Speed Harmonization (DOCA-DSH): This scenario is designed to evaluate the efficiency of the distributed and coordination algorithms for speed harmonization in Chapter 4.
4. Cooperative Signal Timing and Speed Optimization (CSSH): This scenario is designed to coordinate signal controllers with the arrival speed of approaching vehicles.

5.4 Dynamic speed harmonization performance

In this section, the effects of dynamic speed harmonization on network performance are studied. Figure 5-4 shows the time-varying network-level space mean speed for two different scenarios with and without speed harmonization.

When the demand is as low as 500 veh/hr/ln, the network is in uncongested conditions, therefore the speed harmonization strategy increased the average speed at intersection cells for all time periods. Besides, the average speeds on ordinary cells are shown to be less than the not-harmonized cases. The speed harmonization reduces the average speed on the cells before the intersection to adjust the speed of vehicles and prevent unnecessary stops at intersection cells. Reducing the average speed helps reduce the variations of the speeds in the ordinary cells.

When the demand is increased to 900 veh/hr/ln, the network reaches congestion level and speed variations over the network are reduced. Speed harmonization increased the average speeds on the intersection cells in comparison with the not-harmonized case, but the difference of the speeds is less than what was observed in the un-congested conditions. Besides, the average and variation of speed are less at ordinary cells. It should be noted that the simulation starts with

the maximum free-flow speed in the not-harmonized case, and average speeds reduce over time as call occupancy in the network increases.

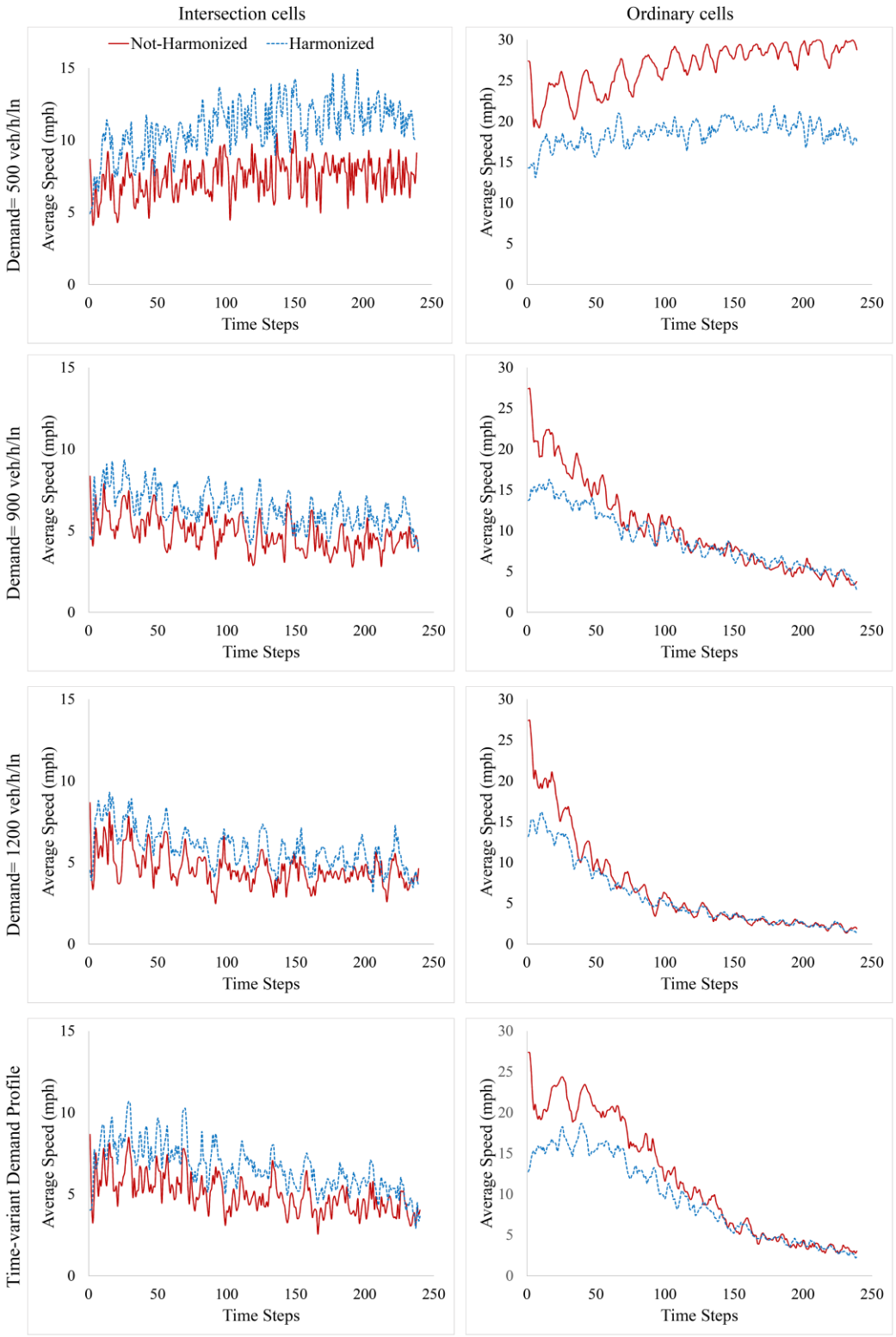

Figure 5.4: **The comparison of speed variations on the network with different demand patterns**

When the network gets more congested (i.e. 1200 veh/hr/ln demand), the average speeds of vehicles for two scenarios are closer to each other because there is not much room to reduce the speed variation. The case with the introduced time-variant demand profile confirms the results of the previous cases as well.

The distribution of average speed over the network is shown in Figure 5-5 for different demand patterns. When the speed is harmonized, the average speed at intersections is higher, while the average speeds are reduced at some links of the network before reaching the intersections to prevent excessive stops at intersections. Moreover, when the network becomes more congested, the average speed decreases in the cases without speed harmonization. However, this reduction is less when the speed harmonization strategy is applied.

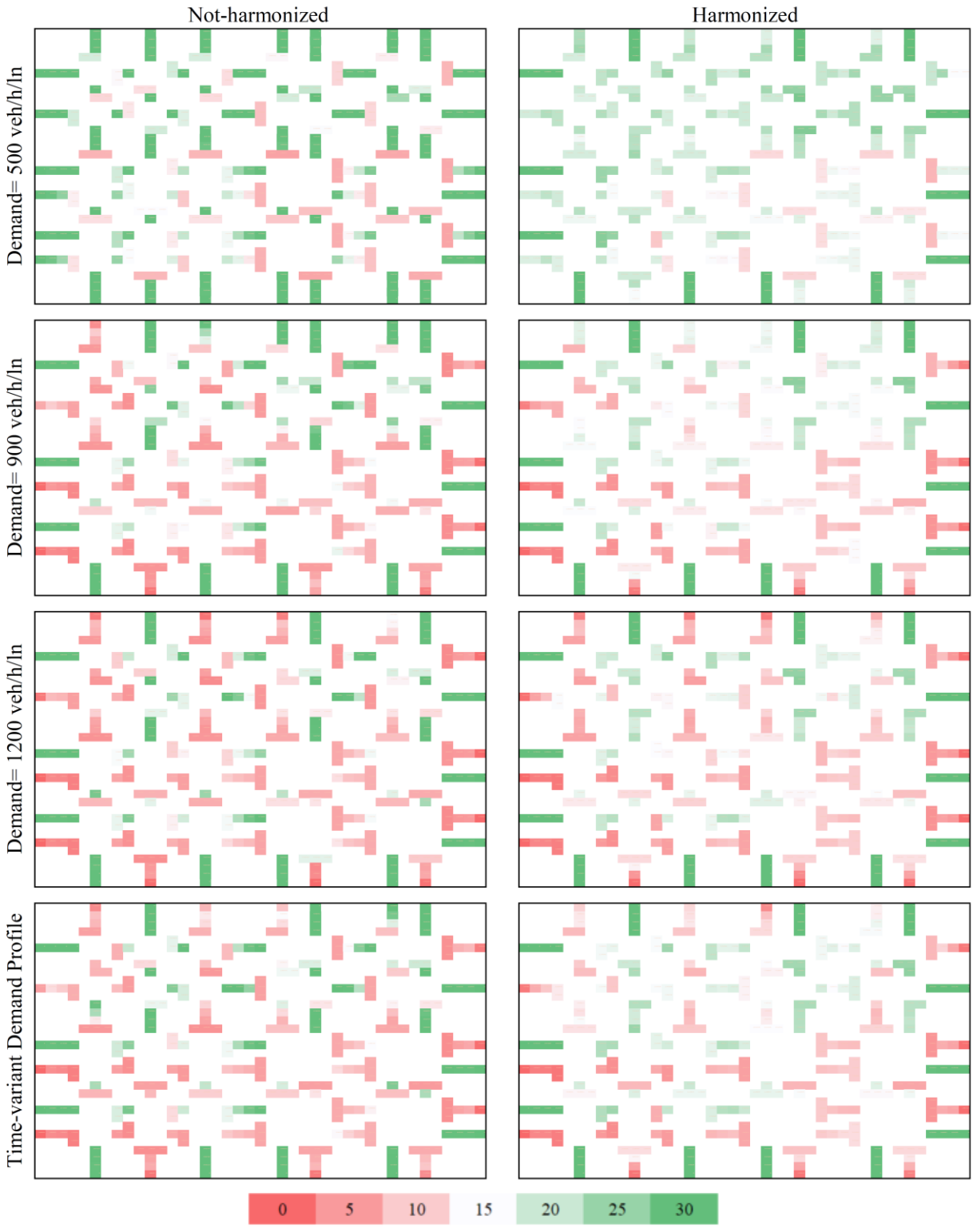

Figure 5.5: **Distribution of the average speed over the network**

As discussed in Chapter 3, there is a trade-off between minimizing the variation of speed and maximizing the throughput in the objective function of the proposed formulation. A series of

sensitivity analyses are performed to find the appropriate value for alpha in the formulation to account for the trade-off. Figure 5-6 shows the variation of the travel time, average speed, and the variance of speed over the entire network. To find the appropriate value for alpha, the trade-off between total travel time and the variance of the speed is considered. As Figure 5-6 illustrates, by increasing the value of alpha, the travel time decreases, and the average speed and variance of space mean speed increase. This observation is expected as higher values of alpha give more weight to maximizing the network throughput, which yields a lower travel time. In addition, we can observe that there is a negative association between travel time and speed variance. We set the value of alpha equal to 0.95 and summarized the mobility performance results in the Springfield network for different demand patterns in Table 5-2.

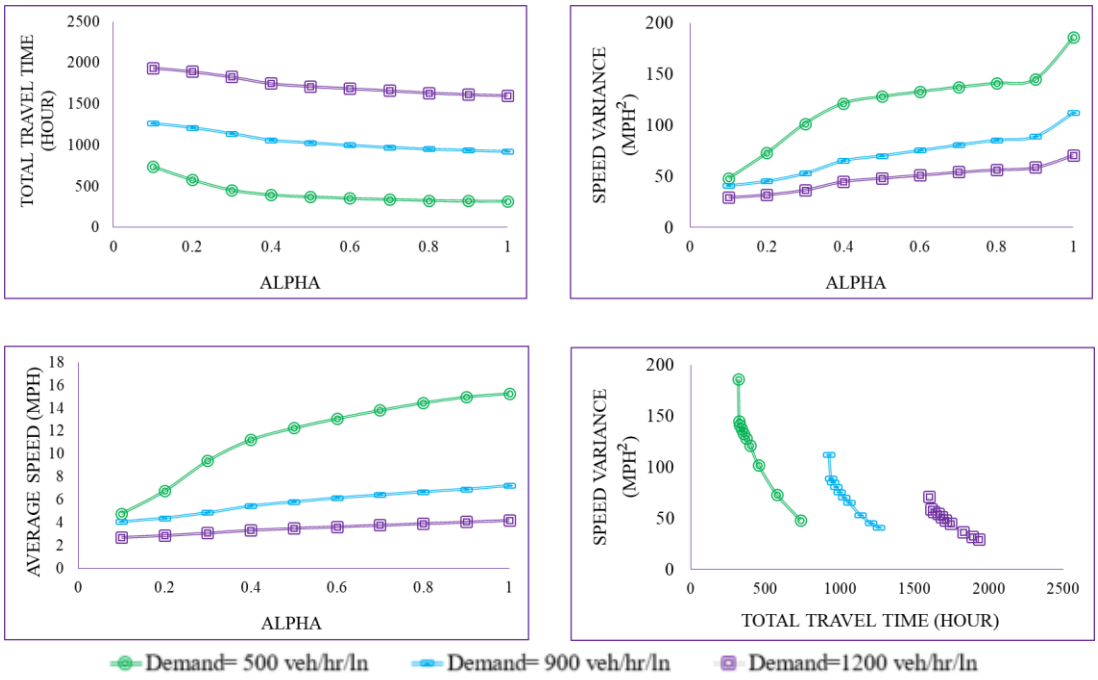

Figure 5.6: **The relationship between travel time, average speed, and speed variance in the network with alpha**

Speed harmonization is less effective when the network is uncongested; because most of vehicles are moving with speeds close to the free-flow speed. As Table 5-2 indicates, the travel time is not reduced when the speed is harmonized in comparison with the non-harmonized case. The average speed and the number of completed trips are reduced slightly. However, the variance of the speed and number of stops are reduced remarkably. As shown in Figure 5-4, speed harmonization increases the average speed at intersection cells in comparison with the not-harmonized case. Therefore, the number of unnecessary stops are decreased. In other words, the number of observations with a space mean speed of zero is decreased, which leads to a reduction in speed variance.

Speed harmonization becomes more effective when the network is in near saturation traffic conditions. When the demand is 900 veh/hr/ln, the total travel time is reduced by about 5.4%. In addition, the average speed and network throughput are increased by 6% and 4%, respectively. The speed variance decreased by 26%. As expected, the number of stops decreased significantly as well.

When traffic demand is 1200 veh/hr/ln, the travel time, speed variance, and number of stops are reduced by 1.5%, 19.8%, and 18.5%, respectively. The same trends were observed with the time-varying demand profile.

Table 5.2: Mobility performance of the network

Demand (veh/hr/ln)	Mobility performance	Harmonized Speed	Not-Harmonized Speed	Difference (%)
500	Travel time (hour)	53.0	53.0	0.0
	Average speed (mph)	15.4	15.6	-1.2
	Variance (mph2)	140.1	198.4	-29.4
	Number of stops	90954.1	99150.4	-8.3
	Number of completed trips	6197.2	6202.2	-0.1
900	Travel time (hour)	155.1	163.9	-5.4
	Average speed (mph)	7.0	6.7	5.9
	Variance (mph2)	90.7	113.7	-20.2
	Number of stops	125560.2	150897.7	-16.8
	Number of completed trips	8032.5	7727.0	4.0
1200	Travel time (hour)	267.8	271.9	-1.5
	Average speed (mph)	4.1	4.1	0.1
	Variance (mph2)	59.33	74.0	-19.8
	Number of stops	127750.2	156695.9	-18.5
	Number of completed trips	7980.2	7857.5	1.6
Time-Variant Demand Profile	Travel time (hour)	168.9	172.5	-2.1
	Average speed (mph)	6.4	6.3	0.5
	Variance (mph2)	87.9	111.5	-21.2
	Number of stops	122948.7	146733.2	-16.2
	Number of completed trips	7850.8	7693.3	2.0

Figures 5-7 show the comparison between the objective function values of DOCA-DSH and the central optimal solutions for the network with twenty intersections. The solutions of DOCA-DSH are at most 2.66% different from the global optimal solutions. The solutions of DOCA-DSH always provide a lower-bound to the DSH problem.

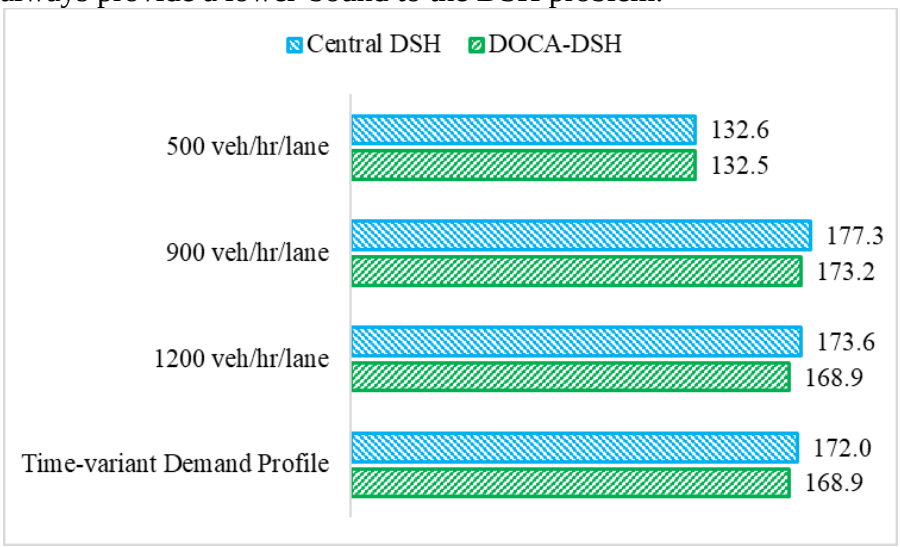

Figure 5.7: **Objective values for different demand patterns in the network with 20 intersections ($\times 10^5$)**

Moreover, we compared the gaps between DOCA-DSH and the central optimal solution in Figure 5-8 when the network size changes. Three networks with eight, twenty, and forty intersections were considered over 250 time steps. The results showed that increasing the demand and network size are associated with higher optimality gaps.

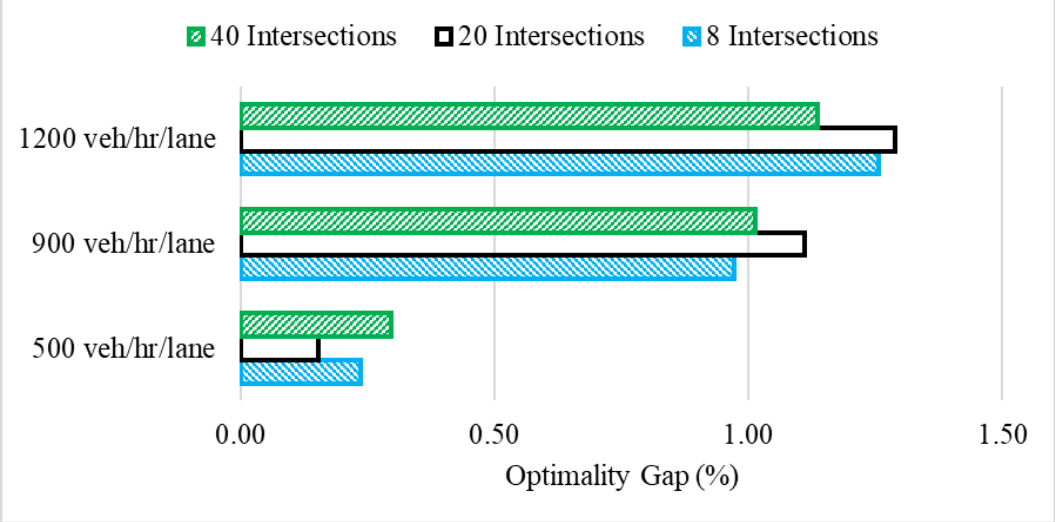

Figure 5.8: **The optimality gap for the networks with different sizes with a study period of 250 time steps**

We increased the study period to 500 time steps in Figure 5-10. The same trends in terms of the optimality gap were observed.

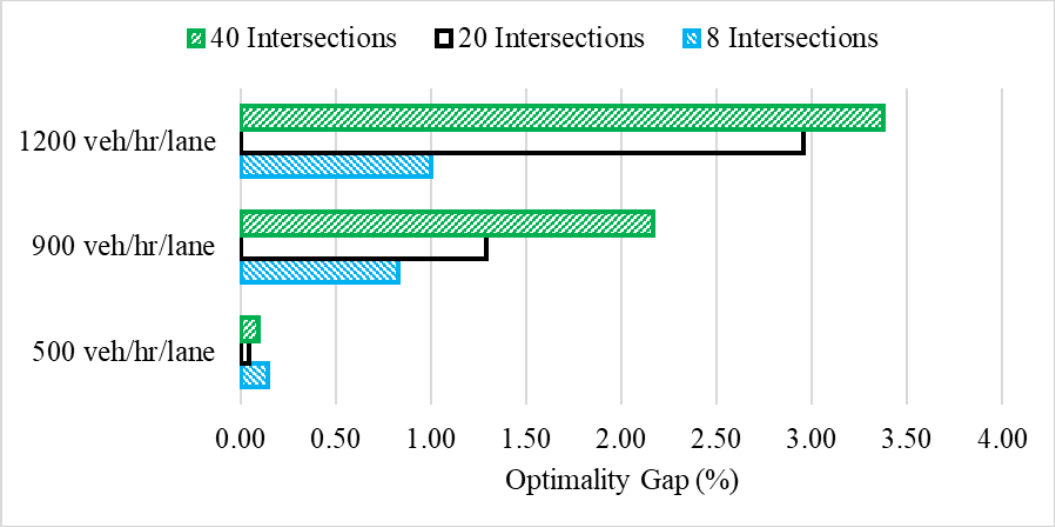

Figure 5.9: **The optimality gap for the networks with different sizes with a study period of 500 time steps**

The runtimes are derived from solving the algorithm using the CPLEX engine in Java environment on a PC with a Core i7 CPU and 24 GB of memory. Figure 5-10 shows the average run time for each DOCA-DSH subproblem. The pattern is the same for all different demand patterns. The highest observed runtime was 0.53 seconds for each time step implementation. As the time step duration is 6 seconds, there is enough time for processing and implementation of the proposed approach in real-time situations.

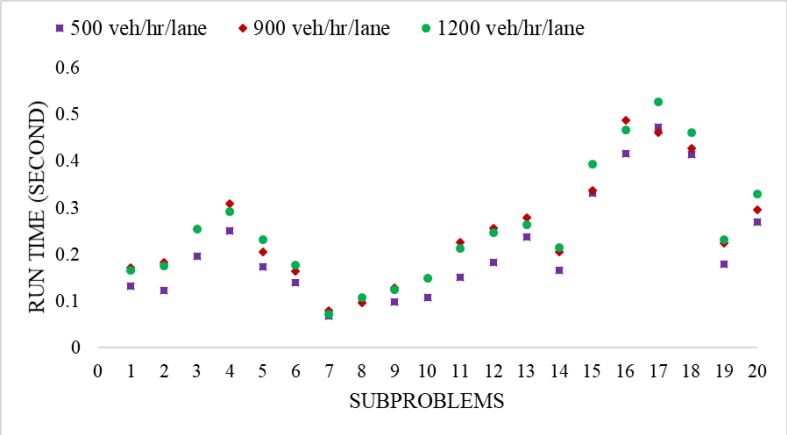

Figure 5.10: **Average runtimes of subproblems**

The runtime is also compared for two different study periods. Table 5-3 shows the total runtime for demand of 900 veh/hour/lane when we compared two cases with 250 and 500 time steps study period. Increasing the study period was associated with the runtime increase. In addition, we observed that there is no association between the size of the network and runtime when the study period is fixed.

Table 5.3: Total runtimes (second) for different sizes and study periods when demand is 900 veh/hour/lane

Network	Time steps	DOCA-DSH	Central DSH	Difference (%)
8 Intersections	250	123.1	120.4	2.3
	500	252.0	643.3	-60.8
20 Intersections	250	125.4	386.5	-67.6
	500	272.0	1601.9	-83.0
40 Intersections	250	132.1	1679.7	-92.1
	500	279.5	12722.9	-97.8

The prediction period of MPC and the size of subproblems are other factors that could affect the runtime. Therefore, we compared the average runtime when subproblems consist of one, two, and three intersections. As Table 5-4 shows, increasing the size of subproblems and prediction period length were associated with higher runtimes.

Table 5.4: Comparing the average runtimes (seconds) for one, two, and three intersection-based subproblems

Prediction period (seconds)	Subproblem size		
	1 Intersection	2 Intersections	3 Intersections
50	0.51	1.64	2.07
100	1.31	3.87	7.08
150	2.23	8.22	13.57

5.5 Coordinated signal timing and speed harmonization performance

The cooperative signal timing and speed harmonization strategy is compared with two other traffic operations strategies to show its effectiveness. The CSSH strategy is compared with

(a) speed harmonization and (b) signal timing optimization. Note that signal parameters are optimized using genetic algorithms (Hajbabaie, Medina and Benekohal, 2010, 2011; Hajbabaie, 2012) for the independent speed harmonization scenario before speed harmonization. Moreover, the desired speed is assumed to be the free flow speed for all vehicles under independent signal timing optimization.

Table 5-5 provides the detailed network performance for CSSH, independent signal timing optimization, and independent speed harmonization strategies in Vissim for the time-variant demand profile (shown in Figure 5-2). It is shown that coordinated signal timing and speed harmonization was able to reduce the travel time, average delay, average number of stops, and average delay at stops respectively by 32.5%, 38%, 35.3%, and 42.1% compared to the independent speed harmonization. Moreover, it increased the network throughput and average speed by 41.4% and 104.2%, respectively. Besides, CSSH could reduce the travel time, average delay, average number of stops, and average delay at stops respectively by 1.9%, 5.3%, 28.5%, and 5.4% compared to the independent signal timing optimization. In addition, network throughput and average speed increased by 1.7% and 3.4%, respectively.

Table 5.5: The network mobility performances for three scenarios and three demand patterns based on Vissim

Mobility performance	Value	(3) CSSH % Diff to (2)	% Diff to (1)	(2) Signal optimization	(1) Speed harmonization
Travel time (hour)	3533.8	-1.9	-32.5	3600.5	5236.7
Throughput (vehicle)	15093	1.7	41.4	14839	10671
Average Delay (sec.)	464.4	-5.3	-38.0	490.5	749.0
Average speed (mph)	3.9	3.4	104.2	3.8	1.9
Average number of stops	12.0	-28.5	-35.3	16.9	18.6
Average delay at stop (sec.)	385.5	-5.4	-42.1	407.5	666.2

Figures 5-11 compare vehicle trajectories between independent signal timing optimization (part a) and cooperative signal timing and speed optimization (part b). The trajectories are plotted for eastbound Washington St. with three lanes, which consists of five intersections. The results show that the movement of vehicles got smoothened and the number of stops was reduced with the CSSH strategy. Moreover, we can observe that vehicles that entered the network at the same time could leave earlier when the CSSH strategy was applied.

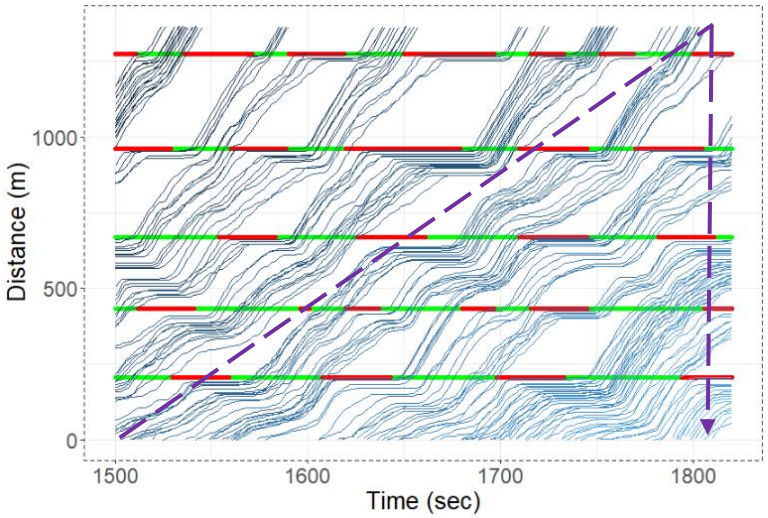

a) Signal timing optimization

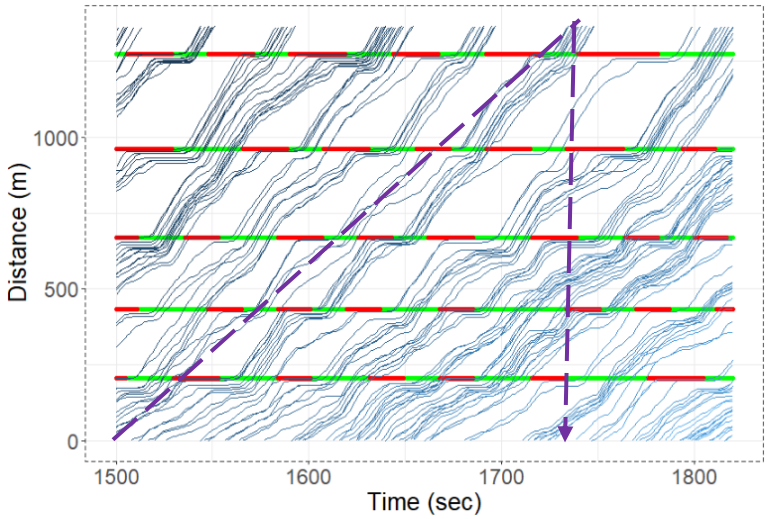

(b) Coordinated signal and speed harmonization

Figure 5.11: **Vehicles** trajectories

We have also shown the optimal signal timing parameters for different movements of intersection number 19 in Figure 5-12. Each movement has received enough green time between the minimum and maximum values. Note that the time step for signal timing is 6 seconds.

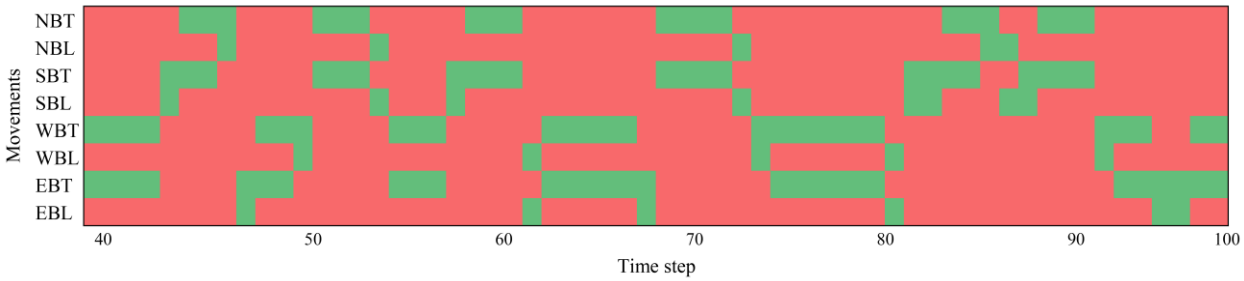

Figure 5.12: **Optimal signal timing parameters at intersection 19**

Figure 5-13 (a)-(c) shows the objective value of CSSH solutions and the corresponding upper bound and lower bounds found by the Benders decomposition (Geoffrion, 1972) in the undersaturated, saturated, and oversteered conditions, respectively. The solution of DOCA is always a lower bound to the global optimal solution since it provides a feasible answer to the maximization problem. Therefore, we measure the optimality gap from the difference of the upper bound found by the Benders decomposition and the solution of DOCA. The maximum optimality gaps observed for the CSSH problem were 4.9%, 5.4%, and 5.2% for the undersaturated, saturated, and oversaturated demand levels, respectively.

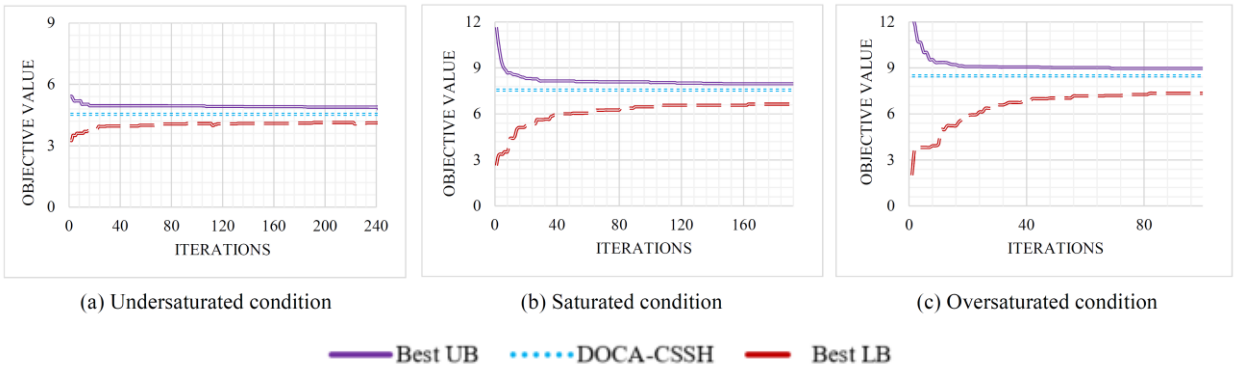

Figure 5.13: **DOCA and the benchmark solutions objective values ($\times 10^5$) for three demand patterns**

The runtimes for the CSSH problem are also provided in Figure 5-14, where a PC with a Core i9 CPU and 64 GB of memory was utilized to solve the problem. The maximum runtime for the mixed-integer problem was 2.45 seconds. This means that the algorithm works in real-time since the implementation period is six seconds.

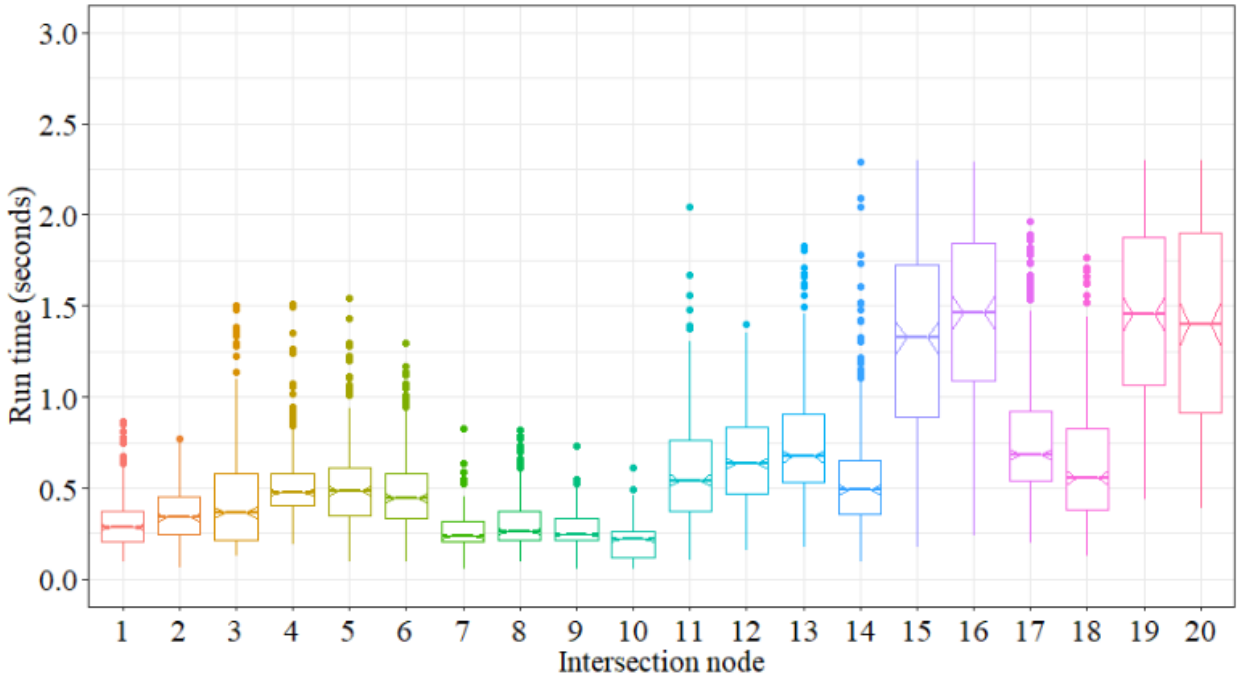

Figure 5.14: **DOCA runtimes at each intersection node.**

Chapter 6. Summary and Conclusions

Connected and automated vehicle technology provides an opportunity to improve traffic operations and reduce travel time in transportation networks. Controlling the speed of vehicles not only increases the network capacity but also improves driving comfort by providing a "smoother" flow of traffic. Dynamic speed harmonization in urban street networks helps adjust the speed of vehicles and consequently their arrival time to signalized intersections. Therefore, the number of stops and unnecessary acceleration/deceleration can be reduced significantly, which leads to a reduction in travel delay and fuel consumption.

This project aimed at evaluating the effectiveness of controlling the speed of connected and automated vehicles in urban transportation networks. We developed a novel methodology for dynamic speed harmonization to improve mobility, especially at signalized intersections. We showed that the proposed problem formulation could significantly improve mobility in transportation networks by decreasing the travel time (up to 5.4%), speed variance (19.8%-29.4%), and number of stops (8.3-18.5%), while increasing the average speed (up to 5.9%) and number of completed trips (up to 4%) in the tested case studies.

This research also showed that traffic operations can be further improved by integrating signal timing optimization into speed harmonization. This approach helps plan vehicle arrival to signalized intersections more accurately, which improves green signal utilization. The results showed that cooperative signal timing and speed harmonization could reduce the average delay by 38% and 5.3% in comparison with only speed optimization and only signal timing optimization, respectively. In addition, the number of stops could be reduced by 35.3% and 28.5%, respectively.

This project studied the effects of speed harmonization on traffic operations. Much research is devoted to travel time reliability (Aghdashi, Rouphail and Hajbabaie, 2013; Zegeer *et al.*, 2014; Aghdashi *et al.*, 2015; Hajbabaie, Aghdashi and Rouphail, 2016). The effects of speed harmonization on travel time reliability is an interesting topic to be researched in future studies.

References

Abdel-Aty, M., Dilmore, J. and Dhindsa, A. (2006) 'Evaluation of variable speed limits for real-time freeway safety improvement', *Accident Analysis & Prevention*, 38(2), pp. 335–345. doi: 10.1016/j.aap.2005.10.010.

Aghdashi, S., Hajbabaie, A., Schroeder, B. J., Trask, J. L. and Rouphail, N. M. (2015) *Generating scenarios of freeway reliability analysis: Hybrid approach*, *Transportation Research Record*. doi: 10.3141/2483-17.

Aghdashi, S., Rouphail, N. M. and Hajbabaie, A. (2013) *Estimation of Incident Propensity for Reliability Analysis in the Highway Capacity Manual*.

Almqvist, S., Hydén, C. and Risser, R. (1991) 'Use of speed limiters in cars for increased safety and a better environment', *Transportation Research Record*, (1318).

Araghi, Sahar and Khosravi, Abbas and Creighton, D. (2015) 'Distributed Q-learning Controller for a Multi-Intersection Traffic Network', in *International Conference on Neural Information Processing*. Springer, pp. 337--344.

Asadi, B. and Vahidi, A. (2010) 'Predictive cruise control: Utilizing upcoming traffic signal information for improving fuel economy and reducing trip time', *IEEE transactions on control systems technology*. IEEE, 19(3), pp. 707–714.

Aziz, H. M. A. and Ukkusuri, S. V. (2012) 'Integration of Environmental Objectives in a System Optimal Dynamic Traffic Assignment Model', *Computer-Aided Civil and Infrastructure Engineering*, 27(7), pp. 494–511. doi: 10.1111/j.1467-8667.2012.00756.x.

Borrough, P. (1997) 'Variable speed limits reduce crashes significantly in the UK', *The Urban Transportation Monitor*.

Boyd, S., Parikh, N., Chu, E., Peleato, B. and Eckstein, J. (2011) 'Distributed optimization and statistical learning via the alternating direction method of multipliers', *Foundations and Trends{®} in Machine Learning*. Now Publishers Inc., 3(1), pp. 1–122. doi: 10.1561/2200000016.

Camacho, E. F. and Bordons, C. (2012) *Model predictive control in the process industry*. Springer Science & Business Media.

Daganzo, C. F. (1994) 'The cell transmission model: A dynamic representation of highway traffic consistent with the hydrodynamic theory', *Transportation Research Part B: Methodological*, 28(4), pp. 269–287.

Feng, Y., Head, K. L., Khoshmagham, S. and Zamanipour, M. (2015) 'A real-time adaptive signal control in a connected vehicle environment', *Transportation Research Part C: Emerging Technologies*. Elsevier Ltd, 55, pp. 460–473. doi: 10.1016/j.trc.2015.01.007.

Geoffrion, A. M. (1972) ‘Generalized Benders decomposition’, *Journal of Optimization Theory and Applications*. Kluwer Academic Publishers-Plenum Publishers, 10(4), pp. 237–260.

Grumert, E., Ma, X. and Tapani, A. (2015) ‘Analysis of a cooperative variable speed limit system using microscopic traffic simulation’, *Transportation Research Part C: Emerging Technologies*, 52, pp. 173–186. doi: 10.1016/j.trc.2014.11.004.

Ha, T.-J., Kang, J.-G. and Park, J.-J. (2003) ‘The effects of automated speed enforcement systems on traffic-flow characteristics and accidents in Korea’, *Institute of Transportation Engineers. ITE Journal*. Institute of Transportation Engineers, 73(2), p. 28.

Hajbabaie, A. (2012) *Intelligent dynamic signal timing optimization program*. University of Illinois at Urbana-Champaign.

Hajbabaie, A., Aghdashi, S. and Rouphail, N. M. (2016) ‘Enhanced decision-making framework using reliability concepts for freeway facilities’, *Journal of Transportation Engineering*, 142(4). doi: 10.1061/(ASCE)TE.1943-5436.0000797.

Hajbabaie, A. and Benekohal, Rahim (2011) ‘Does traffic metering improve network performance efficiency?’, in *IEEE Conference on Intelligent Transportation Systems, Proceedings, ITSC*, pp. 1114–1119.

Hajbabaie, A. and Benekohal, R. (2011) ‘Which policy works better for signal coordination? Common, or variable cycle length’, in *Proceedings of the 1st ASCE T&DI Congress*, pp. 13–16.

Hajbabaie, A. and Benekohal, R. (2013) ‘Traffic signal timing optimization: Choosing the objective function’, *Transportation Research Record: Journal of the Transportation Research Board*. Transportation Research Board of the National Academies, pp. 10--19.

Hajbabaie, A. and Benekohal, R. F. (2015) ‘A Program for Simultaneous Network Signal Timing Optimization and Traffic Assignment’, *IEEE Transactions on Intelligent Transportation Systems*, 16(5), pp. 2573–2586. doi: 10.1109/TITS.2015.2413360.

Hajbabaie, A., Medina, J. C. and Benekohal, R. F. (2010) ‘Effects of ITS-Based Left Turn Policies on Network Performance’, in *IEEE Conference on Intelligent Transportation Systems, Proceedings, ITSC*, pp. 80–84.

Hajbabaie, A., Medina, J. C. and Benekohal, R. F. (2011) ‘Traffic signal coordination and queue management in oversaturated intersections’, *Purdue University Discovery Park*.

Hajbabaie, A. and Mohebifard, R. (2020) *Dynamic Metering in Connected Urban Street Networks: Improving Mobility*.

Hajibabai, L., Bai, Y. and Ouyang, Y. (2014) ‘Joint optimization of freight facility location and pavement infrastructure rehabilitation under network traffic equilibrium’, *Transportation Research Part B: Methodological*. Elsevier, 63, pp. 38–52.

Hajibabai, L. and Ouyang, Y. (2013) ‘Integrated planning of supply chain networks and

multimodal transportation infrastructure expansion: model development and application to the biofuel industry', *Computer-Aided Civil and Infrastructure Engineering*. Wiley Online Library, 28(4), pp. 247–259.

Hajibabai, L. and Ouyang, Y. (2016) 'Dynamic Snow Plow Fleet Management Under Uncertain Demand and Service Disruption', *IEEE Transactions on Intelligent Transportation Systems*. IEEE, 17(9), pp. 2574–2582.

Hajibabai, L. and Saha, D. (2019) 'Patrol route planning for incident response vehicles under dispatching station scenarios', *Computer-Aided Civil and Infrastructure Engineering*. Wiley Online Library, 34(1), pp. 58–70.

Hao, P., Wu, G., Boriboonsomsin, K. and Barth, M. J. (2015) 'Developing a framework of eco-approach and departure application for actuated signal control', in *Intelligent Vehicles Symposium (IV), 2015 IEEE*, pp. 796–801.

He, Q., Head, K. L. and Ding, J. (2014) 'Multi-modal traffic signal control with priority, signal actuation and coordination', *Transportation Research Part C: Emerging Technologies*. Elsevier Ltd, 46, pp. 65–82. doi: 10.1016/j.trc.2014.05.001.

He, X., Liu, H. X. and Liu, X. (2015) 'Optimal vehicle speed trajectory on a signalized arterial with consideration of queue', *Transportation Research Part C: Emerging Technologies*, 61, pp. 106–120. doi: 10.1016/j.trc.2015.11.001.

Hegyi, A., De Schutter, B. and Hellendoorn, H. (2005) 'Model predictive control for optimal coordination of ramp metering and variable speed limits', *Transportation Research Part C: Emerging Technologies*, 13(3), pp. 185–209.

HomChaudhuri, B., Vahidi, A. and Pisu, P. (2015) 'A fuel economic model predictive control strategy for a group of connected vehicles in urban roads', in *2015 American Control Conference (ACC)*, pp. 2741–2746.

Islam, S., Aziz, H. and Hajbabaie, A. (2020) 'Stochastic Gradient-Based Optimal Signal Control With Energy Consumption Bounds', *IEEE Transactions on Intelligent Transportation Systems*, pp. 1–14.

Islam, S. and Hajbabaie, A. (2017) 'Distributed coordinated signal timing optimization in connected transportation networks', *Transportation Research Part C: Emerging Technologies*, 80, pp. 272–285. doi: 10.1016/j.trc.2017.04.017.

Islam, S., Hajbabaie, A. and Aziz, H. (2020) 'A Real-Time Network-Level Traffic Signal Control Methodology with Partial Connected Vehicle Information', *Transportation Research Part C: Emerging Technologies*, 121(102830).

Jung, H., Choi, S., Park, B. B., Lee, H. and Son, S. H. (2016) 'Bi-level optimization for eco-traffic signal system', in *Connected Vehicles and Expo (ICCVE), 2016 International Conference on*, pp. 29–35.

Kamalanathsharma, R. K., Rakha, H. A. and Yang, H. (2015) 'Networkwide Impacts of Vehicle Ecospeed Control in the Vicinity of Traffic Signalized Intersections', *Transportation Research Record: Journal of the Transportation Research Board*. Transportation Research Board of the National Academies, (2503), pp. 91–99.

Kaths, J. (2016) 'Integrating reliable speed advisory information and adaptive urban traffic control for connected vehicles', in *Transportation Research Board 95th Annual Meeting*.

Khondaker, B. and Kattan, L. (2015) 'Variable speed limit: A microscopic analysis in a connected vehicle environment', *Transportation Research Part C: Emerging Technologies*, 58, pp. 146–159. doi: 10.1016/j.trc.2015.07.014.

Letter, C. and Elefteriadou, L. (2017) 'Efficient control of fully automated connected vehicles at freeway merge segments', *Transportation Research Part C: Emerging Technologies*. Elsevier, 80, pp. 190–205.

Levin, M. W. and Boyles, S. D. (2016) 'A cell transmission model for dynamic lane reversal with autonomous vehicles', *Transportation Research Part C: Emerging Technologies*. Elsevier, 68, pp. 126–143.

Li, M., Wu, X., He, X., Yu, G. and Wang, Y. (2018) 'An eco-driving system for electric vehicles with signal control under V2X environment', *Transportation Research Part C: Emerging Technologies*. Elsevier, 93, pp. 335–350.

Li, Z., Elefteriadou, L. and Ranka, S. (2014) 'Signal control optimization for automated vehicles at isolated signalized intersections', *Transportation Research Part C: Emerging Technologies*. Elsevier, 49, pp. 1–18.

MacDonald, M. (2008) 'ATM Monitoring and Evaluation, 4-Lane Variable Mandatory Speed Limits 12 Month Report (Primary and Secondary Indicators)', *Published by Department of Transport*.

Malikopoulos, A. A., Hong, S., Lee, J. and Park, B. B. (2016) 'Development and Evaluation of Speed Harmonization Using Optimal Control Theory', *arXiv preprint arXiv:1611.04647*.

Mandava, S., Boriboonsomsin, K. and Barth, M. (2009) 'Arterial velocity planning based on traffic signal information under light traffic conditions', in *Intelligent Transportation Systems, 2009. ITSC'09. 12th International IEEE Conference on*, pp. 1–6.

Medina, J. C., Hajbabaie, A. and Benekohal, R. F. (2010) 'Arterial traffic control using reinforcement learning agents and information from adjacent intersections in the state and reward structure', in *13th International IEEE Conference on Intelligent Transportation Systems*, pp. 525–530.

Medina, J. C., Hajbabaie, A. and Benekohal, R. F. (2011) 'A comparison of approximate dynamic programming and simple genetic algorithm for traffic control in oversaturated conditions - Case study of a simple symmetric network', in *IEEE Conference on Intelligent Transportation Systems, Proceedings, ITSC*, pp. 1815–1820.

Medina, J., Hajbabaie, A. and Benekohal, R. (2013) 'Effects of metered entry volume on an oversaturated network with dynamic signal timing', *Transportation Research Record: Journal of the Transportation Research Board*. Transportation Research Board of the National Academies, pp. 53--60.

Mehrabipour, M. and Hajbabaie, A. (2017) 'A Cell Based Distributed-Coordinated Approach for Network Level Signal Timing Optimization', *Computer Aided Civil and Infrastructure Engineering: an International Journal*, 32(7), pp. 599–616.

Mehrabipour, M., Hajibabai, L. and Hajbabaie, A. (2019) 'A decomposition scheme for parallelization of system optimal dynamic traffic assignment on urban networks with multiple origins and destinations', *Computer-Aided Civil and Infrastructure Engineering*.

Mirheli, Amir and Hajibabai, L. (2020) 'Charging Infrastructure and Pricing Strategy: How to Accommodate Different Perspectives?', in *The IEEE 23rd International Conference on Intelligent Transportation Systems (ITSC)*.

Mirheli, A and Hajibabai, L. (2020) 'Utilization Management and Pricing of Parking Facilities Under Uncertain Demand and User Decisions', *IEEE Transactions on Intelligent Transportation Systems*, 21(5), pp. 2167–2179.

Mirheli, A., Hajibabai, L. and Hajbabaie, A. (2018) 'Development of a signal-head-free intersection control logic in a fully connected and autonomous vehicle environment', *Transportation Research Part C: Emerging Technologies*, 92, pp. 412–425. doi: 10.1016/j.trc.2018.04.026.

Mirheli, A., Tajalli, M., Hajibabai, L. and Hajbabaie, A. (2019) 'A consensus-based distributed trajectory control in a signal-free intersection', *Transportation Research Part C: Emerging Technologies*, 100, pp. 161–176. doi: 10.1016/j.trc.2019.01.004.

Misener, J., Shladover, S. and Dickey, S. (2010) 'Investigating the Potential Benefits of Broadcasted Signal Phase and Timing (SPAT) Data under IntelliDriveSM', in *ITS America Annual Meeting, Houston, Texas*.

Mohebifard, R. and Hajbabaie, A. (2018) 'Dynamic traffic metering in urban street networks: Formulation and solution algorithm', *Transportation Research Part C: Emerging Technologies*, 93, pp. 161–178. doi: 10.1016/j.trc.2018.04.027.

Mohebifard, R. and Hajbabaie, A. (2019a) 'Distributed Optimization and Coordination Algorithms for Dynamic Traffic Metering in Urban Street Networks', *IEEE Transactions on Intelligent Transportation Systems*, 20(5), pp. 1930–1941. doi: 10.1109/TITS.2018.2848246.

Mohebifard, R. and Hajbabaie, A. (2019b) 'Optimal network-level traffic signal control: A benders decomposition-based solution algorithm', *Transportation Research Part B: Methodological*, 121, pp. 252–274. doi: 10.1016/j.trb.2019.01.012.

Mohebifard, R., Islam, S. and Hajbabaie, A. (2019) 'Cooperative traffic signal and perimeter control in semi-connected urban-street networks', *Transportation Research Part C: Emerging*

Technologies, 104, pp. 408–427. doi: 10.1016/j.trc.2019.05.023.

Niroumand, R., Tajalli, M., Hajibabai, L. and Hajbabaie, A. (2020a) 'Joint optimization of vehicle-group trajectory and signal timing: Introducing the white phase for mixed-autonomy traffic stream', *Transportation Research Part C: Emerging Technologies*. Elsevier, 116, p. 102659.

Niroumand, R., Tajalli, M., Hajibabai, L. and Hajbabaie, A. (2020b) 'The Effects of the "White Phase" on Intersection Performance with Mixed-Autonomy Traffic Stream', in *The 23rd IEEE International Conference on Intelligent Transportation Systems*. IEEE.

Ntousakis, I. A., Nikolos, I. K. and Papageorgiou, M. (2016) 'Optimal vehicle trajectory planning in the context of cooperative merging on highways', *Transportation Research Part C: Emerging Technologies*. Elsevier, 71, pp. 464–488.

PTV Group (2013) 'PTV Vissim 7 User Manual', *PTV AG*.

Robinson, M. D. (2000) 'Examples of variable speed limit applications'.

Sanchez, M., Cano, J. and Kim, D. (2006) 'Predicting traffic lights to improve urban traffic fuel consumption', in *ITS Telecommunications Proceedings, 2006 6th International Conference on*, pp. 331–336.

Smulders, S. (1990) 'Control of freeway traffic flow by variable speed signs', *Transportation Research Part B: Methodological*. Elsevier, 24(2), pp. 111–132.

Tajalli, M. and Hajbabaie, A. (2018a) 'Distributed optimization and coordination algorithms for dynamic speed optimization of connected and autonomous vehicles in urban street networks', *Transportation Research Part C: Emerging Technologies*, 95, pp. 497–515. doi: 10.1016/j.trc.2018.07.012.

Tajalli, M. and Hajbabaie, A. (2018b) 'Dynamic Speed Harmonization in Connected Urban Street Networks', *Computer-Aided Civil and Infrastructure Engineering*, 33(6), pp. 510–523. doi: 10.1111/mice.12360.

Tajalli, M., Mehrabipour, M. and Hajbabaie, A. (2020) 'Network-Level Coordinated Speed Optimization and Traffic Light Control for Connected and Automated Vehicles', *IEEE Transactions on Intelligent Transportation Systems*, pp. 1–12. doi: 10.1109/TITS.2020.2994468.

Taylor, P., Papageorgiou, M. and Mayr, R. (2007) 'Optimal decomposition methods applied to motorway traffic control', (November 2014), pp. 37–41. doi: 10.1080/00207178208922618.

Tettamanti, T. and Varga, I. (2010) 'Distributed traffic control system based on model predictive control', 1, pp. 3–9.

Timotheou, S., Panayiotou, C. G. and Polycarpou, M. M. (2015) 'Distributed Traffic Signal Control Using the Cell Transmission Model via the Alternating Direction Method of Multipliers', 16(2), pp. 919–933.

Wan, N., Vahidi, A. and Luckow, A. (2016) ‘Optimal speed advisory for connected vehicles in arterial roads and the impact on mixed traffic’, *Transportation Research Part C: Emerging Technologies*. Elsevier.

Wang, S. (2013) ‘Efficiency and equity of speed limits in transportation networks’, *Transportation Research Part C: Emerging Technologies*, 32, pp. 61–75. doi: 10.1016/j.trc.2013.04.003.

van de Weg, G. S., Hegyi, A., Hoogendoorn, S. P. and De Schutter, B. (2015) ‘Efficient model predictive control for variable speed limits by optimizing parameterized control schemes’, in *2015 IEEE 18th International Conference on Intelligent Transportation Systems*, pp. 1137–1142.

Wei, Y., Avc\i, C., Liu, J., Belezamo, B., Ayd\in, N., Li, P. T. and Zhou, X. (2017) ‘Dynamic programming-based multi-vehicle longitudinal trajectory optimization with simplified car following models’, *Transportation research part B: methodological*. Elsevier, 106, pp. 102–129.

Xia, H., Boriboonsomsin, K. and Barth, M. (2013) ‘Dynamic eco-driving for signalized arterial corridors and its indirect network-wide energy/emissions benefits’, *Journal of Intelligent Transportation Systems*. Taylor & Francis, 17(1), pp. 31–41.

Xia, H., Boriboonsomsin, K., Schweizer, F., Winckler, A., Zhou, K., Zhang, W.-B. and Barth, M. (2012) ‘Field operational testing of eco-approach technology at a fixed-time signalized intersection’, in *2012 15th International IEEE Conference on Intelligent Transportation Systems*, pp. 188–193.

Xu, B., Ban, X. J., Bian, Y., Li, W., Wang, J., Li, S. E., Member, S. and Li, K. (2018) ‘Cooperative Method of Traffic Signal Optimization and Speed Control of Connected Vehicles at Isolated Intersections’, *IEEE Transaction on Intelligent Transportation Systems*. IEEE, PP, pp. 1–14. doi: 10.1109/TITS.2018.2849029.

Yan, C.-Y., Jiang, R., Gao, Z.-Y. and Shao, H. (2015) ‘Effect of speed limits in degradable transport networks’, *Transportation Research Part C: Emerging Technologies*, 56, pp. 94–119. doi: 10.1016/j.trc.2015.03.042.

Yang, Y., Lu, H., Yin, Y. and Yang, H. (2013) ‘Optimization of variable speed limits for efficient, safe, and sustainable mobility’, *Transportation Research Record: Journal of the Transportation Research Board*. Transportation Research Board of the National Academies, (2333), pp. 37–45.

Zegeer, J., Bonneson, J., Dowling, R., Ryus, P., Vandehey, M., Kittelson, W., Rouphail, N., Schroeder, B., Hajbabaie, A., Aghdashi, B. and others (2014) *Incorporating Travel Time Reliability into the Highway Capacity Manual*.

Zhu, F. and Ukkusuri, S. V. (2014) ‘Accounting for dynamic speed limit control in a stochastic traffic environment: A reinforcement learning approach’, *Transportation Research Part C: Emerging Technologies*, 41, pp. 30–47. doi: 10.1016/j.trc.2014.01.014.

Zhu, F. and Ukkusuri, S. V. (2015) ‘A linear programming formulation for autonomous

intersection control within a dynamic traffic assignment and connected vehicle environment', *Transportation Research Part C: Emerging Technologies*, 55, pp. 363–378. doi: 10.1016/j.trc.2015.01.006.